Bone Marrow Transplantation (2004) 34, 595–602

www.nature.com/bmt

Recovery of Vα24$^+$ NKT cells after hematopoietic stem cell transplantation

K Haraguchi[1,2,3], T Takahashi[1], K Hiruma[2], Y Kanda[1], Y Tanaka[2], S Ogawa[1], S Chiba[1], O Miura[3], H Sakamaki[2] and H Hirai[1,4]

[1]*Department of Hematology and Oncology, Graduate School of Medicine, University of Tokyo, Bunkyo-ku, Tokyo, Japan;* [2]*Hematopoietic Cell Transplantation Team, Tokyo Metropolitan Komagome Hospital, Bunkyo-ku, Tokyo, Japan; and* [3]*Department of Hematology and Oncology, Graduate School of Medicine, Tokyo Medical and Dental University, Bunkyo-ku, Tokyo, Japan*

Summary:

Human Vα24$^+$ natural killer T (NKT) cells have an invariant T-cell receptor-α chain and are activated in a CD1d-restricted manner. Vα24$^+$ NKT cells are thought to regulate immune responses and to play important roles in the induction of allograft tolerance. In this report, we analyzed the recovery of Vα24$^+$ NKT cells after hematopoietic stem cell transplantation and its correlation with graft-versus-host disease (GVHD). Patients who received a dose-reduced conditioning regimen, antithymocyte globulin- or CAMPATH-1H-containing conditioning regimen were excluded. NKT cells were reconstituted within 1 month after transplantation in peripheral blood stem cell transplantation recipients, while their numbers remained low for more than 1 year in bone marrow transplantation (BMT) recipients. The number of Vα24$^+$ NKT cells in BMT recipients with acute GVHD was lower than that in patients without acute GVHD, and both the CD4$^+$ and CD4$^-$ Vα24$^+$ NKT subsets were significantly reduced. With regard to chronic GVHD, BMT recipients with extensive GVHD had significantly fewer Vα24$^+$ NKT cells than other patients. Furthermore, the number of CD4$^+$ Vα24$^+$ NKT cells was also significantly reduced in patients with chronic extensive GVHD. Our results raise the possibility that the number of Vα24$^+$ NKT cells could be related to the development of GVHD.

Bone Marrow Transplantation (2004) **34**, 595–602. doi:10.1038/sj.bmt.1704582
Published online 9 August 2004
Keywords: NKT cells; GVHD; immune reconstitution

Immune reconstitution after hematopoietic stem cell transplantation has been studied by many researchers. Natural killer (NK) cells are reconstituted within 1 month. While the number of CD8$^+$ T cells quickly returns to the normal range, the recovery of CD4$^+$ T cells can take a year or more.[1] In recipients of peripheral blood stem cells, T-cell counts are higher than those in marrow recipients in the first year after transplantation. However, there have been no reports on natural killer T- (NKT) cell reconstitution after hematopoietic stem cell transplantation.[2]

NKT cells are a population of T cells that have NK cell markers such as NK1.1 (NKR-P1C) in mice or CD161 (NKR-P1A) in humans. Most NKT cells use an invariant T-cell receptor (TCR)-α chain (Vα14-Jα18 in mice, Vα24-Jα18 in humans) paired with Vβ8, Vβ7, or Vβ2 in mice, or with Vβ11 in humans.[3–7] Human invariant Vα24$^+$ NKT cells as well as mouse invariant Vα14$^+$ NKT cells are activated by synthetic glycolipids such as α-galactosylceramide in a CD1d-restricted manner. NKT cells produce both Th1 (such as interferon (IFN)-β or tumor necrosis factor (TNF)-α) and Th2 (such as interleukin (IL)-4, IL-5, IL-10, IL-13) cytokines. They can control immune responses to infection and some tumors.[8,9] On the other hand, it is thought that their natural physiological role is immunoregulation, such that they regulate autoimmune diseases or allograft rejection.[8,9]

Graft-versus-host disease (GVHD) is one of the most important complications of hematopoietic stem cell transplantation. It has been shown in a mouse acute GVHD model that bone marrow NK1.1$^+$ T cells can suppress GVHD.[10] It has also been reported that CD8$^+$, CD1d-independent NKT cells, can reduce GVHD in mice.[11] However, there have been no reports on whether or not invariant NKT cells can regulate GVHD.

In this report, we analyzed the recovery of human Vα24$^+$ NKT cells after hematopoietic stem cell transplantation and its correlation with GVHD.

Patients, materials, and methods

Patients and donors

The patients' characteristics are shown in Table 1. They all gave their written informed consent to participate in the study. The procedures were approved by our institutional

Correspondence: Dr K Haraguchi, Department of Hematology and Oncology, Graduate School of Medicine, University of Tokyo, 7-3-1 Hongo, Bunkyo-ku, Tokyo 113-8655, Japan.
E-mail: kyoh-tky@umin.ac.jp
[4]Hisamaru Hirai died on August 23, 2003, during the preparation of this manuscript.
Received 9 January 2004; accepted 14 April 2004
Published online 9 August 2004

Table 1 Patients' characteristics

	BMT, n = 81(32)[a]	*PBSCT, n = 25(7)*
Related/unrelated	14(4)/67(28)	25(7)/0
HLA full match/1 locus mismatch	63(22)/18(10)	23(5)/2(2)
Male/female	52(21)/29(11)	13(4)/12(3)
Age (years)		
Range	16–55	17–53
Median	39	33
Diagnosis		
ALL	17	9
AML	24	8
MLL	1	0
ATL	1	0
CML	16	3
MDS	12	2
MM	2	0
MPD	1	0
NHL	3	3
AA	4	0
Conditioning regimen		
TBI-containing regimen	45(19)	14(4)
No TBI regimen	36(13)	11(3)
GVHD prophylaxis		
Cyclosporine + short-term MTX	69(27)	25(7)
Tacrolimus + short-term MTX	12(5)	0
Acute GVHD		
Grade 0	15	10
Grade I	13	6
Grade II	15	2
Grade III	5	0
Grade IV	1	0
Days to the onset of acute GVHD		
Range	7–73	5–53
Median	13	14
Chronic GVHD		
No	20(13)	6(1)
Limited	11(6)	5(4)
Extensive	16(13)	2(2)
Days to the onset of chronic GVHD		
Range	60–300	110–264
Median	140	200
CMV viremia	20(2)	4
Relapse	13(7)	7(2)

ALL = acute lymphoblastic leukemia; AML = acute myelogenous leukemia; MLL = acute mixed lineage leukemia; ATL = adult T-cell leukemia; CML = chronic myelogenous leukemia; MDS = myelodysplastic disease; MM = multiple myeloma; MPD myeloproliferative disease; NHL = non-Hodgkin lymphoma; AA = aplastic anemia; MTX = methotrexate; CMV = cytomegalovirus.
[a]Numbers within parentheses indicate patients from whom blood samples we could not take during acute phase.

review board. The patients received allogeneic bone marrow transplantation (BMT) or allogeneic peripheral blood stem cell transplantation (PBSCT) at the University of Tokyo Hospital or the Tokyo Metropolitan Komagome Hospital from March 2000 to September 2003. Blood samples were obtained on days 30, 60, 90, and 120–150 in the acute phase, and from 150 to 1155 in the chronic phase after transplantation. Patients who received a dose-reduced conditioning regimen, antithymocyte globulin- or a CAMPATH-1H-containing conditioning regimen were excluded from this study. Patients who received a second transplantation were also excluded. None of the patients received T-cell-depleted grafts.

The normal range for the number of invariant NKT cells in peripheral blood was determined by examining 30 male and 30 female healthy volunteers.

Flow cytometry analysis

Mononuclear cells were separated from blood samples by density-gradient centrifugation (Lymphoprep; AXIS-SHIELD PoC AS, Oslo, Norway). Cells were stained with fluorochrome-conjugated monoclonal antibodies (anti-CD3-FITC (clone UCHT1), anti-CD4-PC5 (clone 13B8.2), anti-TCR Vα24-FITC (clone C15), and anti-TCR Vβ11-PE (clone C21) (Immunotech, Marseille, France) and analyzed by a FACSCalibur apparatus using CellQuest software following the manufacturer's protocol (Becton Dickinson, San Jose, CA, USA). Lymphocytes were gated on forward- and side-scatter plots and the percentage of each lymphocyte subset was determined. The absolute lymphocyte count was determined by a clinical blood test. Each absolute lymphocyte subset count was calculated as the absolute lymphocyte count multiplied by the percentage of the lymphocyte subset divided by 100.

Chimerism of NKT Cells

Genomic DNA was extracted from Vα24 and Vβ11 double-positive cells, which were sorted from the peripheral blood of the recipients (by FACSVantage (Becton Dickinson)) and subjected to a short tandem repeat (STR)-PCR analysis as described previously.[12] Briefly, an STR fragment (D20S471 for pts. 002, 013, and 014, and D22S684 for pt. 003) that showed different allelic polymorphism in a given donor/recipient pair was PCR amplified from extracted DNA and analyzed by an ABI PRISM 377 DNA sequencer in combination with Genescan 3.1 software (Applied Biosystems, Foster City, CA, USA), with which different polymorphic peaks were separated and quantified to evaluate chimerism. Primer sequences were 5′-FAM GGGATGCAGAAATTGCAGTA and TTTTCTCTTTGCCACTGACC for D20S471, and 5′-HEX CCCTCTCCCTCTCTTACAGG and TTCTTAGT GGGGAAGGGATC for D22S684.

Statistical analysis

A statistical analysis was performed with the nonparametric Mann–Whitney *U*-test. A *P*-value of less than 0.05 was considered significant.

Results

Frequency of Vα24+ NKT cells in healthy donors

To measure Vα24+ NKT cells, we counted double-positive cells (Figure 1a). Previous reports have shown that such

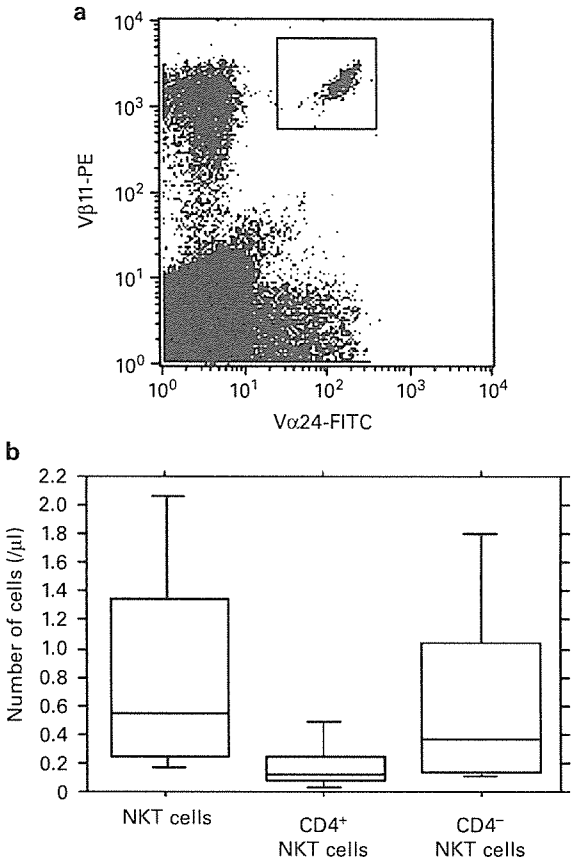

Figure 1 Frequency of Vα24+ NKT cells in healthy donors. (**a**) To measure Vα24+ NKT cells, we counted Vα24 and Vβ11 double-positive cells. The results of flow cytometry on a sample from a healthy donor with a Vα24+ NKT cell count of 0.543/μl are shown. Peripheral blood mononuclear cells from healthy donors (male: $n=30$; female: $n=30$) were stained by three-color fluorescence (Vα24-FITC/Vβ11-PE/CD4-PC5) and analyzed by flow cytometry. Lymphocytes were gated on forward- and side-scatter plots and the ratio of Vα24/Vβ11 cells for each lymphocyte subset was determined. The absolute lymphocyte count was determined by a clinical blood test. (**b**) Composite box plots for the numbers of NKT cells in healthy donors are shown for all Vα24+ NKT cells, CD4+ Vα24+ NKT cells, and CD4− Vα24+ NKT cells. These and all subsequent box plots show the median (horizontal line), 25th and 75th percentiles (box), and 10th and 90th percentiles (error bars). Statistical analysis was performed with the nonparametric Mann–Whitney *U*-test in all subsequent box plots.

cells have invariant TCR-α chain expression[13,14] and are CD1d dependent.[15,16]

The normal range of Vα24+ NKT cells is shown in Figure 1b. The values of the 25th, 50th, and 75th percentiles were 0.239, 0.552, and 1.345/μl, respectively. The median number as a percentage of total mononuclear cells was 0.026%, which was similar to the values in the previous reports.[16–18]

Number of Vα24+ NKT cells varied according to the graft source

There was a significant difference in the number of reconstituted NKT cells between BMT and PBSCT in the acute phase (Figure 2a) and chronic phase (data not shown). In univariate and multivariate analyses, the only variable associated with the number of NKT cells was the stem cell source (PB or BM) in the acute phase. In the chronic phase, similar results were obtained in a univariate analysis, but not in a multivariate analysis. (Variables evaluated included stem cell source (PB or BM, sibling or unrelated), diagnosis, HLA disparity, GVHD prophylaxis, with or without cytomegalovirus (CMV) viremia, GVHD, and with or without steroid treatment.) Since chronic-phase samples were collected between 150 and 1155 days after transplantation, the univariate and multivariate analyses also included time post transplant, but this was not considered as a variable. In BMT, NKT cells were not reconstituted within a year (Figure 2b). In contrast, the number of NKT cells was within the normal range at 1 month after PBSCT (Figure 2c). It was unclear as to whether the number of NKT cells in BMT patients would reach the normal range after 1 year.

We could analyze the chimerism of NKT cells in only four patients in the chronic phase (one received PBSCT and the others received BMT) by PCR-based assays of polymorphic STR markers. They all showed <10% recipient chimerism.

Number of Vα24+ NKT cells in patients with GVHD was lower than that in patients without GVHD in BMT

Since the number of NKT cells in patients who received related BMT was not significantly different from that in patients who received unrelated BMT (data not shown), we analyzed related and unrelated BMT together. The number of Vα24+ NKT cells in BMT recipients without acute GVHD was significantly higher than that in BMT recipients with acute GVHD (Figure 3a). Patients with GVHD were treated with steroids in many cases. Since lymphocytes are decreased when steroids are administered, the treatment of GVHD might reduce the number of NKT cells. However, the administration of steroids to patients with or without GVHD did not significantly affect the number of NKT cells (Figure 3b). In addition, since Vα24+ NKT cells almost universally express inflammatory lymphocyte chemokine receptors, and these receptors may cause them to be distributed at sites of inflammation,[18] they may have been removed from the blood in GVHD patients. However, there was no correlation between CMV viremia and the number of NKT cells (Figure 3c). Most of the Vα24+ NKT subsets are CD4−CD8− (double-negative: DN) and CD4+, although there is a small subset of the CD8+ phenotype in peripheral blood.[14] Since there are so few CD8+ NKT cells and since they are so similar to DN NKT cells,[14] we examined CD4+ and CD4− NKT cells. Both CD4+ and CD4− Vα24+ NKT cells were significantly reduced in patients with acute GVHD (Figure 3d,e). Since there were so few patients with grade III or IV GVHD, we could not evaluate whether or not the severity of GVHD was correlated with the number of NKT cells.

Beyond 150 days after BMT, the number of Vα24+ NKT cells in chronic extensive GVHD patients was significantly lower than that in patients who had no or limited chronic GVHD (Figure 4a). Furthermore, there were significantly fewer CD4+ Vα24+ NKT cells in chronic extensive GVHD

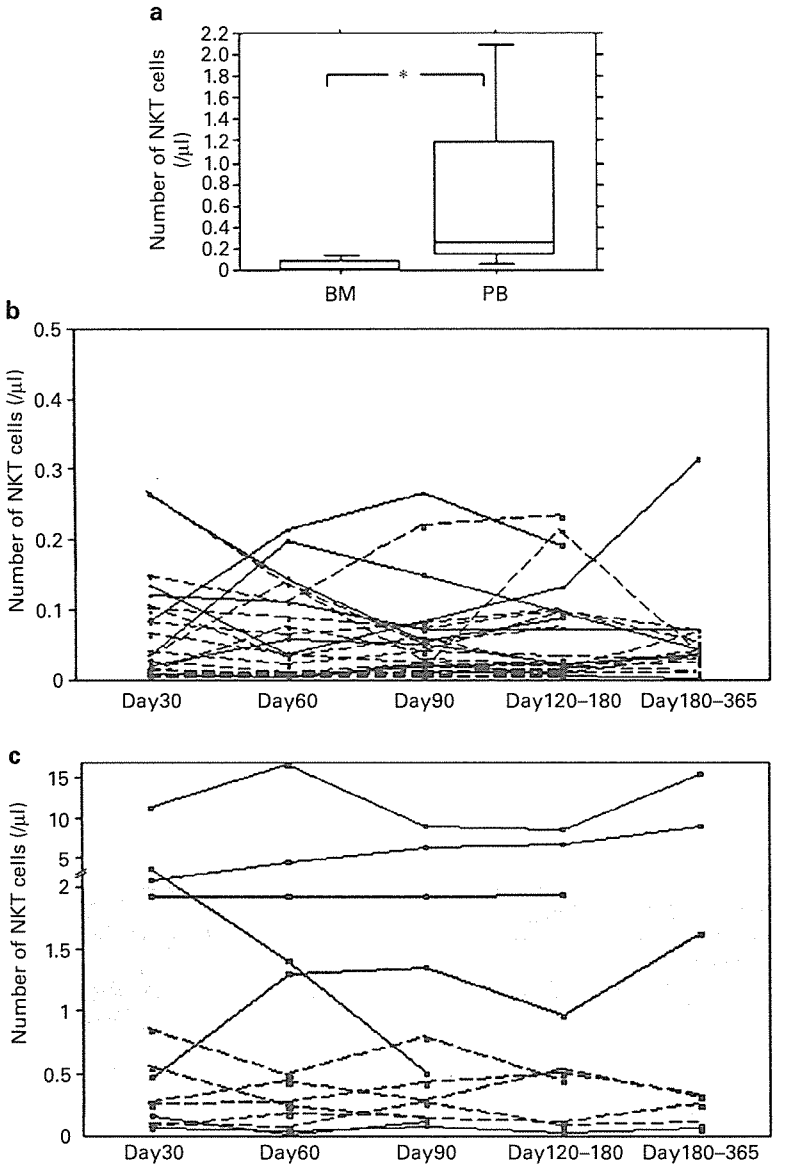

Figure 2 NKT cell recovery in BMT and PBSCT recipients. (**a**) Composite box plots for NKT on day 30 in BMT ($n=41$) and PBSCT ($n=18$). The number of NKT cells in patients who received PBSCT is significantly higher than that in patients who received BMT ($P<0.0001$). (**b** and **c**) NKT cell recovery in BMT (**b**) and PBSCT (**c**) patients. Lines show the individual recovery of NKT cells. Solid lines and closed circles show recovery in patients without GVHD. Dashed lines and open circles show recovery in patients with GVHD. We only show recovery in patients for whom blood samples could be obtained over four times (BMT) or over three times (PBSCT). The figure shows eight (BMT, without GVHD), 20 (BMT, with GVHD), seven (PBSCT, without GVHD), and six patients (PBSCT, with GVHD). The shaded gray area represents the 10–90th percentile values of normal controls.

patients than in other patients (Figure 4b). There were also fewer $CD4^-$ $V\alpha24^+$ NKT cells in chronic extensive GVHD patients, but this difference was not significant (Figure 4c). Again, the administration of steroids did not significantly affect the number of NKT cells (data not shown). Since the generation of murine $V\alpha14^+$ NKT cells is thought to be thymus dependent,[9] NKT cell reconstitution in humans may also be thymus dependent. However, the number of NKT cells did not correlate with the number of CD3 T cells (Figure 4d).

In PBSCT recipients, NKT cell counts in patients with GVHD were not significantly different than those in patients without GVHD (data not shown), although the number of NKT cells in patients without GVHD tended to be higher than that in patients with GVHD (Figure 2c).

As shown in Figure 2b, few GVHD patients with a normal NKT cell count on day 30 subsequently fell outside the normal range, and some patients showed the reverse trend (ie an abnormal NKT count became normal). Therefore, we examined NKT cell recovery and the timing of GVHD or other complications. Figure 5a shows NKT cell recovery in a 30-year-old male who received related BMT. He suffered from gut stage 3 acute GVHD. It was most severe on days 50 and 75, but subsided beginning on

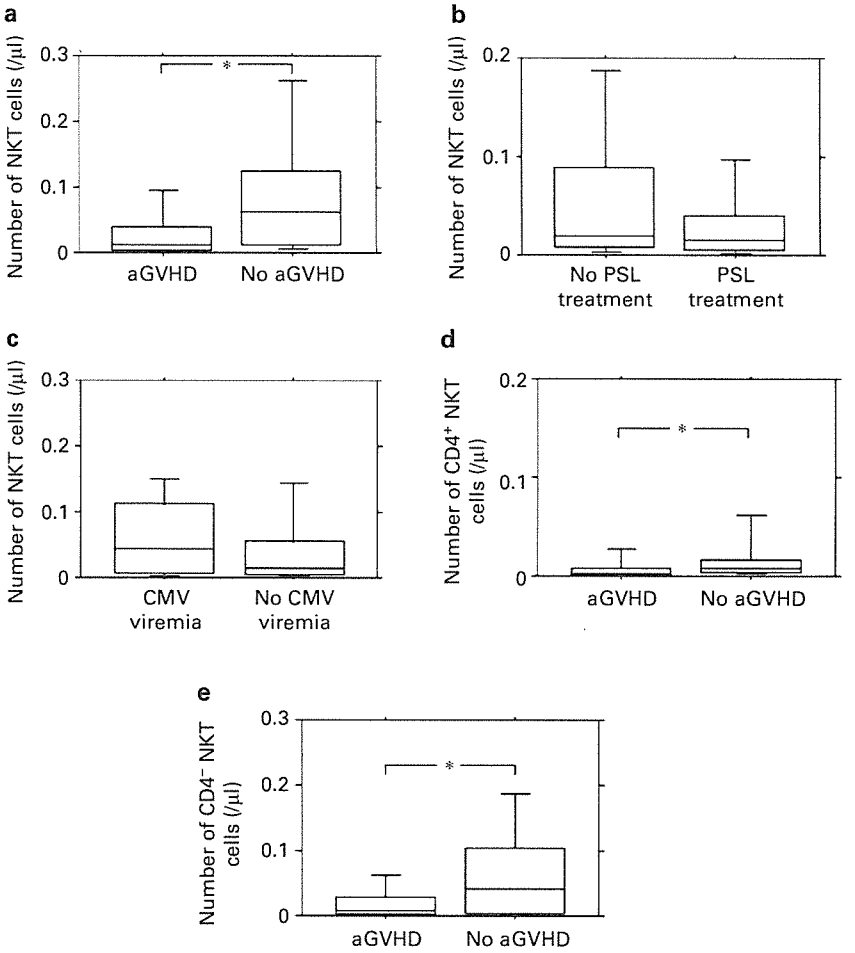

Figure 3 Number of Vα24+ NKT cells in BMT recipients with or without acute GVHD. (**a**) Composite box plots for NKT cells on day 30 in BMT recipients with ($n=24$) or without ($n=24$) acute GVHD The number of Vα24+ NKT cells in BMT recipients without acute GVHD was significantly higher than that in BMT recipients with acute GVHD ($P=0.0172$). (**b**) Composite box plots for NKT cells on day 30 in BMT recipients with acute GVHD who did ($n=22$) or did not ($n=11$) receive steroid treatment. Steroid administration did not affect the number of NKT cells ($P=0.4450$). (**c**) Composite box plots for NKT cells on day 60 in BMT recipients with ($n=14$) or without ($n=30$) CMV viremia. CMV viremia did not affect the number of NKT cells ($P=0.2957$). (**d** and **e**) Composite box plots for CD4+ NKT (**d**) and CD4- NKT (**e**) cells on day 30 in BMT recipients with or without GVHD. Both CD4+ and CD4- Vα24+ NKT cells were significantly reduced in patients with acute GVHD (CD4+: $P=0.0392$; CD4-: $P=0.0337$). *$P<0.05$. aGVHD, acute GVHD.

day 100. Figure 5b shows NKT cell recovery in a 34-year-old female who received unrelated BMT. She suffered from skin stage 3 GVHD on day 10. She received methylprednisolone pulse therapy and recovered quickly. She did not suffer from GVHD afterwards. Figure 5c shows NKT recovery in a 53-year-old female who received unrelated BMT. She suffered from skin stage 3 GVHD on day 17. Her GVHD responded to steroid treatment, but on day 100 she suffered from chronic lung GVHD. All of these cases suggest that GVHD may be correlated with a low number of NKT cells.

Discussion

In this study, we examined the recovery of Vα24+ NKT cells in patients who received hematopoietic stem cell transplantation and its correlation with GVHD. Many studies have suggested that an important physiological function of NKT cells is to control immune responses against infection and some tumors. In transplantation immunity, CD1d-dependent NKT cells are also thought to play a role in the induction of self[19] or allograft[20 22] or xenograft tolerance.[23] In a murine GVHD model, bone marrow DN NK1.1+ T cells were observed to be important for preventing GVHD.[10] Recently, NKT cells that were CD1d independent or that had diverse TCR-α chains have been reported. CD8+ CD1d-independent NKT cells have been shown to reduce GVHD.[11] Bone marrow noninvariant CD1d-restricted NKT cells that had the potential to suppress GVHD have been reported in humans.[17] However, to the best of our knowledge, there has been no previous report that human Vα24+ NKT cells prevented GVHD. In the present study, the number of Vα24+ NKT cells in BMT recipients with acute GVHD or chronic extensive GVHD was lower than that in recipients without

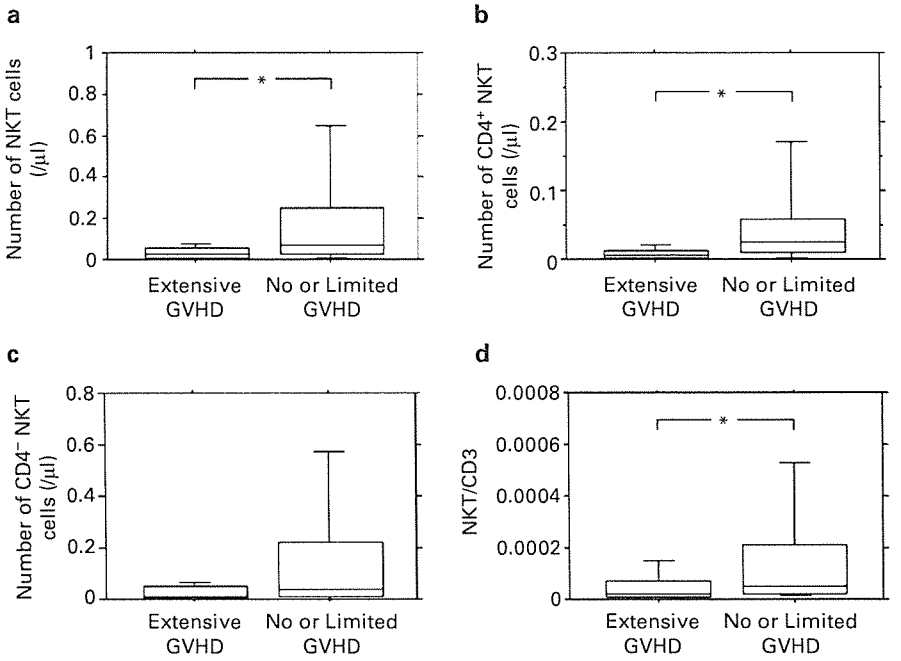

Figure 4 Number of Vα24+ NKT cells in BMT recipients with or without chronic GVHD. (**a**) Composite box plots for NKT in BMT recipients with chronic extensive GVHD ($n=21$) or no or limited chronic GVHD ($n=31$). The number of Vα24+ NKT cells in extensive GVHD patients was significantly lower than that in patients who had no or limited chronic GVHD ($P=0.0089$). (**b** and **c**) Composite box plots for CD4+ Vα24+ (**b**) and CD4- Vα24+ (**c**) NKT cell counts in BMT recipients with extensive chronic GVHD or no or limited chronic GVHD. Chronic extensive GVHD patients had significantly fewer CD4+ and CD4- Vα24+ NKT cells than other patients. However, there was no significant difference in the CD4- Vα24+ NKT cell count (CD4+ NKT cells: $P=0.0012$; CD4-NKT cells: $P=0.0792$, respectively). (**d**) Composite box plots for the ratio of the NKT cell number to the CD3+CD56- T-cell number. The ratio is smaller in chronic extensive GVHD patients ($n=16$) than in other patients ($n=27$) ($P=0.0148$). cGVHD, chronic GVHD.

GVHD. Thus, Vα24+ NKT cells may also function to suppress GVHD, although it is also possible that GVHD decreases the number of NKT cells. The administration of steroids, which is the most popular therapy for GVHD, did not suppress NKT cells. Moreover, the recovery of other lymphocytes (NK cells, B cells, CD4+ T cells, CD8+ T cells, CD4+CD45RA+ T cells, and CD4+CD45RO+ T cells) was not significantly affected by the presence of acute or chronic GVHD (data not shown). Therefore, the low number of NKT cells in patients with GVHD did not result from a delay in lymphocyte recovery. Further analyses using animal models are needed to determine whether the reduced number of NKT cells is a cause or an effect of GVHD.

NKT cells consist of three subsets: DN, CD4+, and CD8+ cells. CD4+ NKT cells produce large amounts of IL-4, while CD4- (DN and CD8+) NKT cells selectively produce Th1 cytokines.[14,15,24] The numbers of both CD4+ and CD4- NKT cells were reduced in acute GVHD patients. It has been suggested that the Th1/Th2 balance influences the development of acute GVHD. For example, there are some reports that Th1 cells cause acute GVHD more efficiently than Th2 cells, and that Th2 cells suppress GVHD.[25-27] Other data have suggested that Th1 cytokines reduced acute GVHD or that Th2 cytokines worsened acute GVHD.[28-30] In any case, it may be important to regulate both Th1 and Th2 cytokines to control GVHD, and thus CD4+ and CD4- Vα24+ NKT cells likely play some roles in preventing acute GVHD.

In the case of chronic GVHD, there were significantly fewer CD4+ Vα24+ NKT cells in patients with chronic extensive GVHD than in those with no or limited GVHD. There also tended to be fewer CD4- Vα24+ NKT cells in chronic extensive GVHD patients, although this difference was not significant. In some reports, Th2 cytokines have been recognized as the principal mediators of chronic GVHD.[19,26] The protective effect against GVHD was strictly dependent on IL-4 production from NKT cells.[10,31] Moreover, CD4+ Vα24+ NKT cells produce large amounts of IL-10,[25,32] and NKT cell-derived IL-10 was essential for the differentiation of antigen-specific regulatory T cells in systemic tolerance.[33] Thus, CD4+ NKT cells that produce Th2 cytokines may suppress the Th1 response and control GVHD.

Recent reports have shown that CD4+CD25+ T cells suppress GVHD.[34] CD4+CD25+ T cells are known to be immune regulatory cells and are essential for the induction and maintenance of self-tolerance and for the protection of autoimmunity. We failed to show that the number of CD4+CD25+ T cells correlated with GVHD (data not shown). CD25 is also expressed when CD4+ T cells are activated in GVHD. Therefore, it might be difficult to count only suppressor T cells.

In Japan, PBSCT is only available to patients who have a related donor, and thus BMT is performed for patients with an unrelated donor. On the other hand, many related hematopoietic stem cell transplantations are PBSCT (we think that this is why the incidence of relapse in the PBSCT

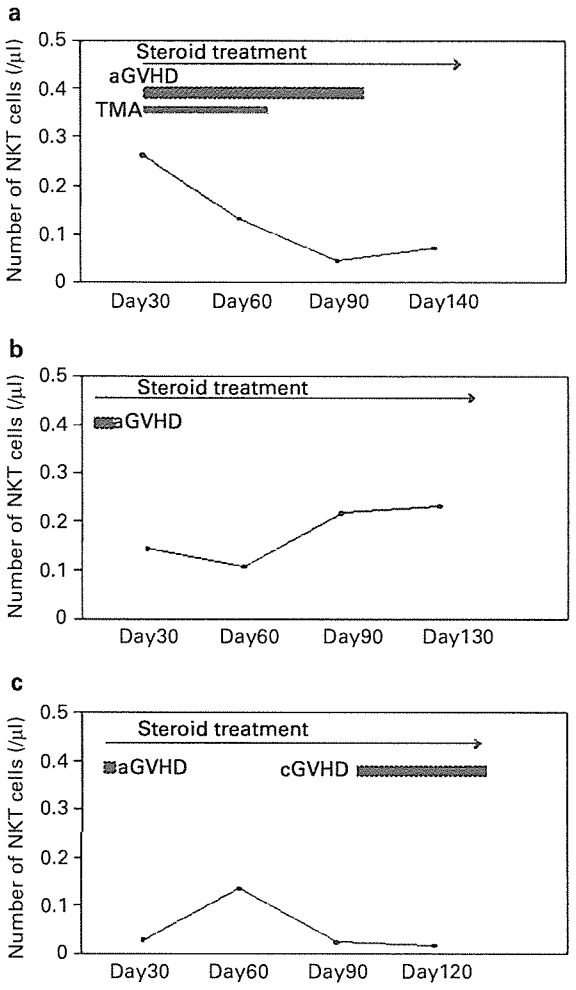

Figure 5 NKT cell recovery and the clinical course in three BMT recipients. (**a**) A 30-year-old male who received related BMT. (**b**) A 34-year-old female who received unrelated BMT. (**c**) A 53-year-old female who received unrelated BMT. Details are provided in the text.

group was higher than that in BMT recipients). Therefore, we cannot simply compare the reconstitution of NKT cells between PBSCT and BMT. However, the difference is so significant that we could safely conclude that the recovery of NKT cells in patients who received PBSCT is much faster than that in patients who received BMT. One possible reason is that PBSC grafts contain more NKT cells than BM grafts. A previous report showed that the number of $V\alpha24^+$ invariant NKT cells in BM was comparable to or less than that in peripheral blood mononuclear cells.[17] These findings indicate that PBSC grafts contain many more $V\alpha24^+$ NKT cells than BM grafts. Chimerism of invariant NKT cells in the chronic phase was donor type, but it is difficult to investigate chimerism in the early phase, especially after BMT because there are extremely few invariant NKT cells. In PBSCT, we failed to show that there were significantly fewer NKT cells in patients with GVHD. One possible reason is that there were very few patients in this study and another is that the number of NKT cells varied widely among individuals.

In conclusion, $V\alpha24^+$ NKT cells were reconstituted rapidly in PBSCT recipients and slowly in BMT recipients. The number of $V\alpha24^+$ NKT cells in patients with GVHD was lower than that in patients without GVHD, and the number of $CD4^+$ NKT cells in GVHD patients is especially low. Our results raise the possibility that the therapeutic administration of $V\alpha24^+$ NKT cells or α-galactosylceramide might ameliorate GVHD. Thus, NKT cells should be considered as an exciting new modality of cellular therapy for the regulation of undesirable immune responses.

Acknowledgements

We thank Eri Nagata for providing excellent technical assistance.

References

1 Fujimaki K, Maruta A, Yoshida M *et al.* Immune reconstitution assessed during five years after allogeneic bone marrow transplantation. *Bone Marrow Transplant* 2001; **27**: 1275–1281.
2 Storek J, Dawson MA, Storer B *et al.* Immune reconstitution after allogeneic marrow transplantation compared with blood stem cell transplantation. *Blood* 2001; **97**: 3380–3389.
3 Fowlkes BJ, Kruisbeek AM, Ton-That H *et al.* A novel population of T cell receptor αβ-bearing thymocytes which predominantly express a single Vβ8 gene family. *Nature* 1987; **329**: 251–254.
4 Budd RC, Miescher GC, Howe RC *et al.* Developmentally regulated expression of T cell receptor β chain variable domain is immature thymocytes. *J Exp Med* 1987; **166**: 577–582.
5 Lantz O, Bendelac A. An invariant T cell receptor α chain is used by a unique subset MHC class I-specific $CD4^+$ and $CD4^-CD8^-$T cells in mice and humans. *J Exp Med* 1994; **180**: 1097–1106.
6 Dellabona P, Padovan E, Casorati G *et al.* An invariant Vα-JαQ/Vα11 T cell receptor is expressed in all individuals by clonally expanded $CD4^-CD8^-$ cells. *J Exp Med* 1994; **180**: 1171–1176.
7 Porcelli S, Gerdes D, Fertig AM, Balk SP. Human T cells expressing an invariant Vα24-JαQ TCRα are $CD4^-$ and heterogeneous with respect to TCRβ expression. *Hum Immunol* 1996; **48**: 63–67.
8 Godfrey DI, Hammond KJL, Poulton LD, Baxter AG. NKT cells: facts, functions and fallacies. *Immunol Today* 2000; **21**: 573–583.
9 Joyce S. CD1d and natural T cells: how their properties jump-start the immune system. *Cell Mol Life Sci* 2001; **58**: 442–469.
10 Zeng D, Lewis D, Dejbakhsh-Jones S *et al.* Bone marrow $NK1.1^-$ and $NK1.1^+$ T cells reciprocally regulate acute graft versus host disease. *J Exp Med* 1999; **189**: 1073–1081.
11 Baker J, Verneris MR, Ito M *et al.* Expansion of cytolytic $CD8^+$ natural killer T cells with limited capacity for graft-versus-host disease induction due to interferon γ production. *Blood* 2001; **97**: 2923–2931.
12 Thiede C, Florek M, Bornhäuser M *et al.* Rapid quantification of mixed chimerism using multiplex amplification of short tandem repeat markers and fluorescence detection. *Bone Marrow Transplant* 1999; **23**: 1055–1060.
13 Takahashi T, Nieda M, Koezuka Y *et al.* Analysis of human $V\alpha24^+CD4^+$ NKT cells activated by α-galactosylceramide-

pulsed monocyte-derived dendritic cells. *J Immunol* 2000; **164**: 4458–4464.
14 Takahashi T, Chiba S, Nieda M *et al.* Analysis of human Vα24+CD8+ NKT Cells activated by α-galactosylceramide-pulsed monocyte-derived dendritic cells. *J Immunol* 2002; **168**: 3140–3144.
15 Karadimitris A, Gadola S, Altamirano M *et al.* Human CD1d-glycolipid tetramers generated by *in vitro* oxidative refolding chromatography. *Proc Natl Acad Sci USA* 2001; **98**: 3294–3298.
16 Lee PT, Benlagha K, Teyton L, Bendelac A. Distinct functional lineages of human Vα24 natural killer T cells. *J Exp Med* 2002; **195**: 637–641.
17 Exley MA, Tahir SMA, Cheng O *et al.* A major fraction of human bone marrow lymphocyte are Th2-like CD1d-reactive T cells that can suppress mixed lymphocyte responses. *J Immunol* 2001; **167**: 5531–5534.
18 Kim CH, Johnston B, Butcher EC. Trafficking machinery of NKT cells: shared and differential chemokine receptor expression among Vα24+Vβ11+ NKT cell subsets with distinct cytokine-producing capacity. *Blood* 2002; **100**: 11–16.
19 Sonoda K, Exley M, Snapper S *et al.* CD1-reactive natural killer T cells are required for development of systemic tolerance through an immune-privileged site. *J Exp Med* 1999; **190**: 1215–1225.
20 Seino K, Fukao K, Muramoto K *et al.* Requirement for natural killer T (NKT) cells in the induction of allograft tolerance. *Proc Natl Acad Sci USA* 2001; **98**: 2577–2581.
21 Chargui J, Hase T, Wada S *et al.* NKT cells as nonspecific immune-regulator inducing tolerance in mouse model transplantation. *Transplant Proc* 2001; **33**: 3833–3834.
22 Higuchi M, Zeng D, Shizuru J *et al.* Immune tolerance to combined organ and bone marrow transplants after fractionated lymphoid irradiation involves regulatory NKT cells and clonal deletion. *J Immunol* 2002; **169**: 5564–5570.
23 Ikehara Y, Yasunami Y, Kodama S *et al.* CD4+Vα24 natural killer T cells are essential for acceptance of rat islet xenografts in mice. *J Clin Invest* 2000; **105**: 1761–1767.
24 Gumperz JE, Miyake S, Yamamura T, Brenner MB. Functionally distinct subsets of CD1d-restricted natural killer T cells revealed by CD1d tetramer staining. *J Exp Med* 2002; **195**: 625–636.
25 Teshima T, Ferrara JLM. Understanding the alloresponse: new approaches to graft-versus-host disease prevention. *Semin Hematol* 2002; **39**: 15–22.
26 Ellison CA, Fischer JMM, HayGlass KT, Gartner JG. Murine graft-versus-host disease in an F1-hybrid model using IFN-α gene knockout donors. *J Immunol* 1998; **161**: 631–640.
27 Allen RD, Staley TA, Sidman CL. Differential cytokine expression in acute and chronic murine graft-versus-host-disease. *Eur J Immunol* 1993; **23**: 333–337.
28 Brok HPM, Heidt PJ, van der Meide PH *et al.* Interferon-γ prevents graft-versus-host disease after allogeneic bone marrow transplantation in mice. *J Immunol* 1993; **151**: 6451–6459.
29 Yang YG, Dey BR, Sergio JJ *et al.* Donor-derived interferon γ is required for inhibition of acute graft-versus-host disease by interleukin 12. *J Clin Invest* 1998; **102**: 2126–2135.
30 Murphy WJ, Welniak LA, Taub DD *et al.* Differential effects of the absence of interferon-γ and IL-4 in acute graft-versus-host disease after allogeneic bone marrow transplantation in mice. *J Clin Invest* 1998; **102**: 1742–1748.
31 Lan F, Zeng D, Higuchi M *et al.* Predominance of NK1.1+TCRαβ+ or DX5+TCRαβ+ T cells in mice conditioned with fractionated lymphoid irradiation protects against graft-versus-host disease: 'natural suppressor' cells. *J Immunol* 2001; **167**: 2087–2096.
32 Takahashi T, Nakamura K, Chiba S *et al.* Vα24+ natural killer T cells are markedly decreased in atopic dermatitis patients. *Hum Immunol* 2003; **64**: 586–592.
33 Sonoda K, Faunce DE, Taniguchi M *et al.* NK T cell-derived IL-10 is essential for the differentiation of antigen-specific T regulatory cells in systemic tolerance. *J Immunol* 2001; **166**: 42–50.
34 Taylor PA, Lees CJ, Blazar BR. The infusion of *ex vivo* activated and expanded CD4+CD25+ immune regulatory cells inhibits graft-versus-host disease lethality. *Blood* 2002; **99**: 3493–3499.

The transcriptionally active form of AML1 is required for hematopoietic rescue of the *AML1*-deficient embryonic para-aortic splanchnopleural (P-Sp) region

Susumu Goyama, Yuko Yamaguchi, Yoichi Imai, Masahito Kawazu, Masahiro Nakagawa, Takashi Asai, Keiki Kumano, Kinuko Mitani, Seishi Ogawa, Shigeru Chiba, Mineo Kurokawa, and Hisamaru Hirai

Acute myelogenous leukemia 1 (AML1; runt-related transcription factor 1 [Runx1]) is a member of Runx transcription factors and is essential for definitive hematopoiesis. Although AML1 possesses several subdomains of defined biochemical functions, the physiologic relevance of each subdomain to hematopoietic development has been poorly understood. Recently, the consequence of carboxy-terminal truncation in AML1 was analyzed by the hematopoietic rescue assay of *AML1*-deficient mouse embryonic stem cells using the gene knock-in approach. Nonetheless, a role for specific internal domains, as well as for mutations found in a human disease, of AML1 remains to be elucidated. In this study, we established an experimental system to efficiently evaluate the hematopoietic potential of AML1 using a coculture system of the murine embryonic para-aortic splanchnopleural (P-Sp) region with a stromal cell line, OP9. In this system, the hematopoietic defect of *AML1*-deficient P-Sp can be rescued by expressing AML1 with retroviral infection. By analysis of AML1 mutants, we demonstrated that the hematopoietic potential of AML1 was closely related to its transcriptional activity. Furthermore, we showed that other Runx transcription factors, Runx2/AML3 or Runx3/AML2, could rescue the hematopoietic defect of *AML1*-deficient P-Sp. Thus, this experimental system will become a valuable tool to analyze the physiologic function and domain contribution of Runx proteins in hematopoiesis. (Blood. 2004;104:3558-3564)

Introduction

Acute myelogenous leukemia 1 (AML1)/runt-related transcription factor 1 (Runx1) belongs to a family of transcriptional regulators called Runx, which contain a conserved 128–amino acid Runt domain responsible for sequence-specific DNA binding.[1] Runx proteins make heterodimeric complexes with a partner protein, CBFβ/PEBP2β (core-binding factor β/polyomavirus enhancer–binding protein 2β),[2-4] and this association is essential for its biologic activity.[5-7] There are 3 known mammalian Runx family members: AML1/Runx1, Runx2/AML3, and Runx3/AML2. Typically, Runx functions as a transcriptional activator of target gene expression. Under some conditions, however, it can repress the transcription of specific genes.

AML1 was originally identified on chromosome 21 as the gene that is disrupted in the (8;21)(q22;q22) translocation, which is one of the most frequent chromosome abnormalities associated with human AML.[8,9] Subsequently, AML1 was shown to be one of the most frequent targets of leukemia-associated gene aberrations.[10,11] Moreover, somatic point mutations of the *AML1* gene were also demonstrated in patients with AML and myelodysplastic syndrome (MDS).[12-14] In addition to a role in leukemic transformation, gene-targeting studies in mice have demonstrated that AML1 is essential for early development of definitive hematopoiesis. *AML1*-deficient embryos develop through the yolk sac stage but die around 12 to 13 days of gestation following complete block of fetal liver hematopoiesis.[15,16]

AML1 includes at least 3 alternative splicing forms: AML1a, AML1b, and AML1c.[17] In AML1b and AML1c, the carboxy (C)–terminal to the Runt domain lies in a region that contains sequences of defined biochemical functions, which are absent in AML1a. Several functional domains have been identified in the C-terminal half, such as *trans*-activation domain,[18,19] *trans*-repression domain,[20] and VWRPY motif.[21-23]

During vertebrate embryogenesis, hematopoietic development consists of 2 distinct waves of discrete cellular components known as primitive and definitive hematopoiesis.[24] In mice, the first wave of primitive hematopoiesis, which consists predominantly of a large and nucleated erythroid cell, emerges in the yolk sac at 7.5 embryonic days after coitus (dpc). Then, primitive hematopoiesis begins to be replaced around 9.5 dpc by definitive hematopoiesis, generally described as the second wave. Progenitors for definitive hematopoiesis originate from para-aortic splanchnopleural (P-Sp) region at 7.5 to 9.5 dpc,[25,26] and long-term repopulating hematopoietic stem cells (LTR-HSCs) that can reconstitute adult mice appear in the aorta-gonad-mesonephros (AGM) at 10.5 to 11.5 dpc.[27,28] These cells subsequently colonize the fetal liver, where they expand and differentiate. Active sites for definitive hematopoiesis

From the Departments of Hematology/Oncology and Regeneration Medicine for Hematopoiesis, Graduate School of Medicine, University of Tokyo, Tokyo, Japan; Department of Cell Therapy/Transplantation Medicine, University of Tokyo Hospital, University of Tokyo, Tokyo, Japan; and Department of Hematology, Dokkyo University School of Medicine, Tochigi, Japan.

Submitted April 22, 2004; accepted July 6, 2004. Prepublished online as *Blood* First Edition Paper, July 22, 2004; DOI 10.1182/blood-2004-04-1535.

Supported in part by a Grant-in-Aid for Scientific Research from the Japan Society for the Promotion of Science and by Health and Labour Sciences Research grants from the Ministry of Health, Labour, and Welfare.

An Inside *Blood* analysis of this article appears in the front of this issue.

Reprints: Mineo Kurokawa, Department of Hematology & Oncology, Graduate School of Medicine, University of Tokyo, 7-3-1 Hongo, Bunkyo-ku, Tokyo 113-8655, Japan; e-mail: kurokawa-tky@umin.ac.jp.

The publication costs of this article were defrayed in part by page charge payment. Therefore, and solely to indicate this fact, this article is hereby marked "advertisement" in accordance with 18 U.S.C. section 1734.

are transferred to bone marrow and spleen prior to birth and function throughout life within these organs. Recent studies have shown that AML1 is expressed in the hematopoietic cell clusters within the P-Sp/AGM region and *AML1*-deficient embryos are devoid of these hematopoietic clusters.[29-32]

The hematopoietic defect of *AML1*-deficient mice could be replicated in vitro by several culture systems, including the P-Sp/AGM culture[33,34] and the embryonic stem (ES) cell culture.[35] In these systems, hematopoietic cells are generated in wild-type cultures but not in *AML1*-deficient cultures. Recently, a gene knock-in approach was used to demonstrate rescue in vivo of hematopoiesis from the *AML1*-deficient ES cells.[35,36] This hematopoietic rescue requires the *trans*-activation domain of AML1 but not the C-terminal *trans*-repression subdomain. However, no report has elucidated roles for specific internal domains or disease-related mutations of AML1 in hematopoiesis.

In the present study, we used a coculture system of cells derived from the P-Sp region with a layer of a stromal cell line, OP9, in which hematopoietic cell development of various lineages is efficiently induced.[37] The cultured P-Sp–derived cells show a significant colony-forming activity in semisolid culture with appropriate cytokines, as well as distinct surface expression of hematopoietic markers. In this culture system, *AML1*-deficient P-Sp–derived cells failed to show any hematopoietic activity. This defect was efficiently rescued by reactivating AML1 by retroviral-mediated expression. Using this system, we then examined a hematopoietic potential of a series of AML1 mutants and demonstrated that the hematopoietic rescue of *AML1*-deficient P-Sp regions require transcriptionally active forms of AML1. We also showed that enforced expression of other Runx transcription factors, Runx2/AML3 or Runx3/AML2, could rescue the hematopoietic defect of *AML1*-deficient P-Sp regions. These results provide evidence that transcriptional activity of AML1 is essential for hematopoietic development from P-Sp regions. In addition, this coculture system makes a useful method to determine functional consequences of AML1 on its hematopoietic potential.

Materials and methods

Mice and embryos

AML1-deficient mice were generated as described previously[38] and were crossed onto the C57BL/6 background. To generate embryos, timed matings were set up between $AML1^{+/-}$ males and $AML1^{+/-}$ females. The time at midday (12:00) was taken to be 0.5 dpc for the plugged mice.

In vitro P-Sp culture

P-Sp culture was performed as described previously[39] with a minor modification. In brief, isolated P-Sp regions of 9.5 dpc embryos were dissociated by incubation with 250 U/mL dispase (Godo Shusei, Tokyo, Japan) for 20 minutes and cell dissociation buffer (Gibco BRL, Carlsbad, CA) for 20 minutes at 37°C, washed once in phosphate-buffered saline (PBS), followed by vigorous pipetting. Approximately 5×10^4 P-Sp–derived cells were suspended in 300 μL serum-free StemPro media (Life Technologies, Gaithersburg, MD) supplemented with 50 ng/mL stem cell factor (SCF), 5 ng/mL interleukin (IL3; gifts from Kirin Brewery, Takasaki, Japan), and 10 ng/mL murine oncostatin M (R&D Systems, Minneapolis, MN). Single-cell suspensions were seeded on preplated OP-9 stromal cells in the 24-well plate, followed by incubation at 37°C.

Plasmid construction

The cDNAs of human AML1a, AML1b, and various AML1 mutants were subcloned as *Eco*RI-*Eco*RI fragments into the retrovirus vector pMY/internal ribosomal entry site–enhanced green fluorescent protein (IRES-EGFP; pMY/IG).[40] C-terminal deletion mutants of AML1b, AML1b-R139G, AML1b-S249/266A, and AML1b-K24/43R were constructed as described previously.[13,41-43] For construction of AML1bΔ(205-332), we deleted the *Pvu*II-*Bst*PI fragment from AML1b, filled the resultant plasmid with a Klenow fragment, and religated it. AML1bΔ(181-210) was created by polymerase chain reaction (PCR) with the insertion of a *Bgl*II restriction site to join the fragments. Flag-tagged human Runx2/AML3 cDNA was inserted into the *Bam*HI and the *Eco*RI restriction sites of pMYs/IRES-EGFP (pMYs/IG).[40] Flag-tagged human Runx3/AML2 cDNA was inserted into the *Sac*II and the *Xho*I sites of the same vector.

Retroviral transduction

Plat-E packaging cells[44] (2×10^6) were transiently transfected with 3 μg of AML1, Runx2/AML3, Runx3/AML2, or AML1 mutants; mixed with 9 μL of FuGENE6 (Roche Molecular Biochemicals, Indianapolis, IN); followed by incubation at 37°C. Supernatant containing retrovirus was collected 48 hours after transfection and used immediately for infection. Retroviral transduction to the cells derived from *AML1*-deficient P-Sp regions was performed as described previously with minor modification.[45] In brief, the viral supernatant was added to the P-Sp culture together with 10 μg/mL Polybrene (Sigma, St Louis, MO). After 72 hours of incubation, virus-containing medium was replaced by standard culture medium. The cells were incubated for another 10 days and processed for analysis. To confirm the expression of Runx proteins, NIH3T3 cells were also infected with the same viral supernatants. The number of retrovirus-infected cells was evaluated by the expression of green fluorescent protein (GFP).

Colony-forming cell (CFC) assay

The nonadherent or semiadherent cells rescued from *AML1*-deficient P-Sp regions were used for CFC assay. Cells (6×10^4) were plated into MethoCult3434 medium (StemCell Technologies, Vancouver, BC, Canada) and cultured in a 5% CO_2 incubator at 37°C. Colony types were determined at day 7 by morphologic appearance and by Wright-Giemsa staining of each colony.

Flow cytometry analysis

Flow cytometry analysis was performed in a FACScalibur with the Cellquest program (Becton Dickinson, San Jose, CA) after addition of propidium iodide to exclude dead cells. For surface staining, cell suspensions collected from the P-Sp cultures were incubated on ice for 30 minutes in the presence of various mixtures of labeled monoclonal antibodies. The monoclonal antibodies used were phycoerythrin (PE)–conjugated anti–granulocyte 1 (anti-Gr1), anti–macrophage antigen 1 (anti-Mac1), anti–stem cell antigen 1 (anti-Sca1), allophycocyanin (APC)–conjugated anti-CD45, anti–c-Kit, and biotin-conjugated anti-CD34. Biotinylated antibodies were then counterstained with PE- or APC-conjugated streptavidin. Isotype-matched antibodies conjugated with the appropriate fluorochrome were used as negative controls.

Western blot analysis

Retrovirus-infected NIH3T3 cells were lysed in radioimmunoprecipitation assay (RIPA) buffer.[41] Whole-cell lysates containing 100 μg of proteins were subjected to sodium dodecyl sulfate–polyacrylamide gel electrophoresis (SDS-PAGE) and transferred to a polyvinylidene difluoride membrane (Immobilon; Millipore, Bedford, MA). The membrane was blocked with 10% skim milk, treated with anti-AML1 (PC284L; Oncogene, Cambridge, MA) or anti-Flag (M2; Sigma), washed, and reacted with the rabbit anti–immunoglobulin G (anti-IgG) antibody coupled to horseradish peroxidase. The blot was visualized using the enhanced chemiluminescence (ECL) system (Amersham Pharmacia Biotech, Piscataway, NJ).

Results

Retroviral expression of AML1 rescues hematopoiesis by *AML1*-deficient P-Sp region

AML1-deficient mice die in midgestation as a result of a complete block in fetal liver hematopoiesis, indicating the strict in vivo requirement of AML1 in definitive hematopoiesis. Consistently, the primary culture system of the P-Sp region has demonstrated that the failure of hematopoiesis in the fetal liver is preceded by a hematopoietic defect in the P-Sp region, from which the development of hematopoietic cells was never detected in *AML1*-deficient embryos.[34,35] When the cells isolated from wild-type P-Sp regions at 9.5 dpc were cocultured with OP9 stromal cells, small and round-shaped nonadherent cells were produced in 5 days (Figure 1A). These cells were thought to represent a hematopoietic cell population of various lineages because they expressed hematopoietic cell surface markers and generated hematopoietic cell colonies when plated into a semisolid culture (Figure 2; data not shown). In contrast, the cells from *AML1*-deficient P-Sp regions failed to develop any hematopoietic cells (Figure 1B), which coincides with the notion that AML1 is a prerequisite for hematopoietic cell production in the P-Sp region. Thus, AML1-dependent hematopoiesis could be recapitulated in vitro, and we went on further to examine whether reactivation of a transcriptionally active form of AML1 can rescue this hematopoietic defect. First, by packaging the pMY/IG-AML1b in Plat-E cells, we generated the AML1b-IRES-GFP retrovirus that expresses AML1b and GFP. Then we infected the cells derived from the *AML1*-deficient P-Sp region with the AML1b-IRES-GFP retrovirus and cultured for an additional 10 days. Interestingly, AML1b-infected cultures generated numerous small and round cells with a nonadherent property (Figure 1C). In contrast, cultures infected with the empty vector (control) produced no such cells (Figure 1D). These nonadherent cells were morphologically indistinguishable from the hematopoietic cells generated from the wild-type P-Sp cells and proliferated continuously for more than 30 days. These results suggest that lack of P-Sp hematopoiesis can be complemented by retrovirus-mediated reactivation of AML1 in this culture system.

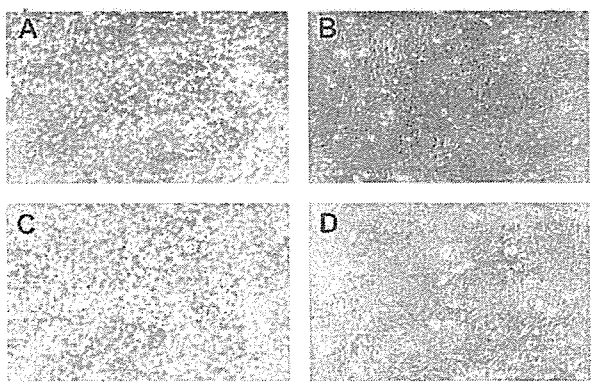

Figure 1. Retroviral expression of AML1b rescues hematopoiesis from *AML1*-deficient P-Sp regions. Photographs were taken with a Nikon Eclipse TE2000-U (Nikon Sanker, Tokyo, Japan) at a magnification of × 100 after 5 days of culture (A-B) and 14 days of culture (C-D). (A) Hematopoietic cells emerged at day 5 from wild-type P-Sp regions. (B) No hematopoietic cells were observed in the culture of *AML1*-deficient P-Sp regions, showing only the background of OP9 cells. (C) AML1b-transduced P-Sp regions from an *AML1*-deficient embryo generated numerous round, nonadherent, or semiadherent cells. (D) A control culture infected with mock virus failed to generate any hematopoietic cells.

Rescued cells retain the features of hematopoietic cells

In the previous study, Mukouyama et al[35] described that the retroviral transfer of AML1 into the *AML1*-deficient P-Sp region gave rise to the production of small and round cells in the culture with an appropriate combination of cytokines. However, under their experimental condition in which no stromal cell layer was employed, the recovered cells showed neither CFC activity nor expression of hematopoietic cell surface markers, such as CD45 and c-Kit, which indicates that the rescue of the hematopoietic defect is incomplete, if it occurs at all. To determine whether the nonadherent cells recovered under our experimental condition retain the features of hematopoietic cells, we examined CFC activity and surface markers of those cells, both of which are distinctly detected in wild-type P-Sp–derived cells in our coculture system. On the 10th day of culture, the nonadherent cells were collected and seeded into a semisolid medium. As shown in Figure 3, these cells generated a number of mixed, granulocyte/macrophage, and erythroid colonies, indicating that the recovered cells should contain various types of CFCs, possibly including definitive lineages. In addition, the flow cytometric analysis revealed that the rescued cells expressed hematopoietic cell surface markers, such as a marker of hematopoietic cells, CD45; myeloid markers Gr1/Mac1; and markers of hematopoietic progenitors c-Kit, Sca1, and CD34 (Figure 2). Their expression profiles were nearly identical to those of hematopoietic cells generated from the wild-type P-Sp cells (Figure 2).

Thus, in contrast to the previous report,[35] we found that the nonadherent cells derived from *AML1*-deficient P-Sp regions in our culture system retained the features of hematopoietic cells that are indistinguishable from those of wild-type P-Sp–derived cells. It is, thus, likely that seeding onto OP9 stromal cells may provide a more favorable environment for production of hematopoietic cells from P-Sp regions and/or the expansion of P-Sp–derived hematopoietic cells.

Hematopoietic potential of AML1 mutants

Using this experimental system, we then analyzed the hematopoietic potential of various AML1 mutants (Figure 4). We generated retroviruses that express a variety of AML1 mutants, including serial C-terminal truncation, deletion of functional domains, and substitution of specific residues. NIH3T3 cells were infected with these viruses and the titer of the retroviruses was evaluated by flow cytometric measurement of GFP-positive NIH3T3 cells (Figure 5A). Coincidently, retrovirus-mediated expression of each mutant in infected cells was confirmed by Western blotting (Figure 5B).

Among those mutants, we first used a series of C-terminal deletion mutants including AML1a and examined their hematopoietic potential by delivering them into the *AML1*-deficient P-Sp region in our coculture system. AML1bΔ444 and AML1bΔ397, which possess the *trans*-activation subdomain, retained the ability to rescue the hematopoietic defect of the *AML1*-deficient P-Sp region (Figure 6A-B). In contrast, AML1bΔ335, AML1bΔ288, and AML1a, which lack the *trans*-activation domain, failed to produce any hematopoietic cells (Figure 6C-E). In addition, AML1bΔ(205-332), which retains the C-terminal region but lacks a half of the activation domain, has also lost the hematopoietic potential (Figure 6G). Thus, consistent with the observation in the previous report,[35] in vitro hematopoietic rescue requires the *trans*-activation domain of AML1, whereas the C-terminal repression domain including VWRPY motif is dispensable for this function.

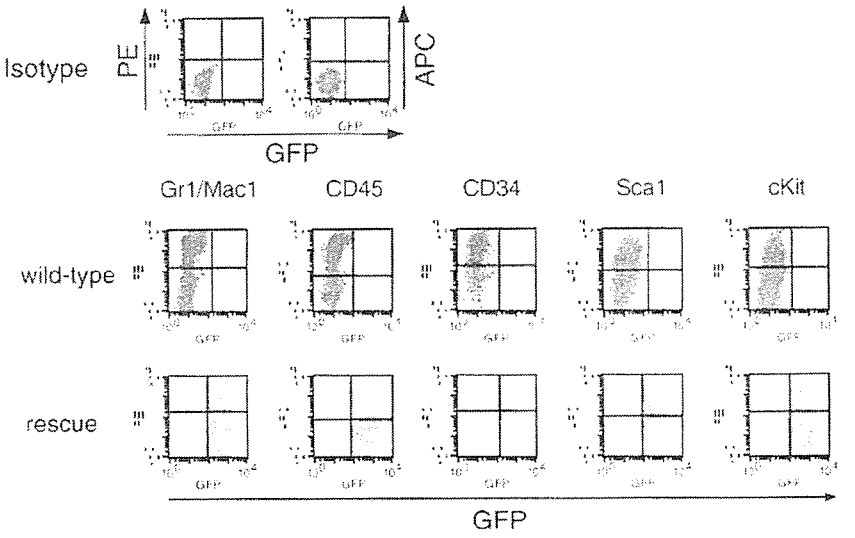

Figure 2. Expression of the hematopoietic markers on the rescued cells from *AML1*-deficient P-Sp culture. Flow cytometric profiles of the cells stained with antibodies against Gr1/Mac1, CD45, CD34, Sca1, and c-Kit. Note that the rescued cells from *AML1*-deficient P-Sp regions are GFP-positive and express various hematopoietic cell surface markers. Flow cytometric profiles of the rescued cells are similar to those of hematopoietic cells in wild-type P-Sp culture. GFP intensity (marking retrovirally transduced cells) is plotted on the x-axis and intensity of counterstaining of hematopoietic surface markers is plotted on the y-axis. Isotype-matched control staining of the hematopoietic cells from wild-type P-Sp regions is also shown.

The Runt domain of AML1 is essential for both DNA binding and heterodimerization with CBFβ, but its role in hematopoietic development has not yet been directly investigated. Therefore, we next examined the hematopoietic potential of AML1bΔRD, a deletion mutant that lacks the Runt domain and is defective for both DNA binding and heterodimerization with CBFβ. As shown in Figure 6F, AML1bΔRD could not rescue hematopoiesis from *AML1*-deficient P-Sp regions, indicating an essential role for the Runt domain in the hematopoietic potential of AML1. To elucidate more explicitly a role of DNA binding of AML1, we used AML1b-R139G, a mutant isolated from a patient with MDS, which harbors point mutation causing substitution of Arg139 in the Runt domain with Gly.[13] The DNA-binding ability is severely impaired in AML1b-R139G, whereas heterodimerization with CBFβ is spared. As shown in Figure 6I, AML1b-R139G also failed to show any hematopoietic potential. These results indicate that DNA binding of AML1 through the Runt domain is also indispensable for in vitro hematopoietic rescue of the *AML1*-deficient P-Sp region.

Among corepressors that are recruited by AML1 is mSin3A, which may contribute to AML1-mediated repression of gene transcription, as well as to intracellular stability of AML1.[20,46] Indeed, the AML1 mutant that cannot interact with mSin3A [AML1bΔ(181-210)] is defective for repression of the *p21* promoter in the in vitro transcription response assay. Posttranscriptional modification is also one of the important mechanisms that regulate AML1 function.[42,43] For example, transcriptional activity of AML1 is enhanced by extracellular signal-regulated kinase (ERK)–dependent phosphorylation on Ser249 and Ser266, whereas p300-mediated acetylation on Lys24 and Lys43 augments DNA binding of AML1. To clarify roles of these regulatory mechanisms in the hematopoietic potential of AML1, we used 3 types of AML1 mutants: AML1bΔ(181-210), AML1b-S249/266A, and AML1b-K24/43R. AML1bΔ(181-210) is an internal deletion mutant that lacks the binding domain for the mSin3A.[20] In AML1b-S249/266A, the 2 target serines for ERK-mediated phosphorylation were replaced with alanines, which results in lack of ERK-induced

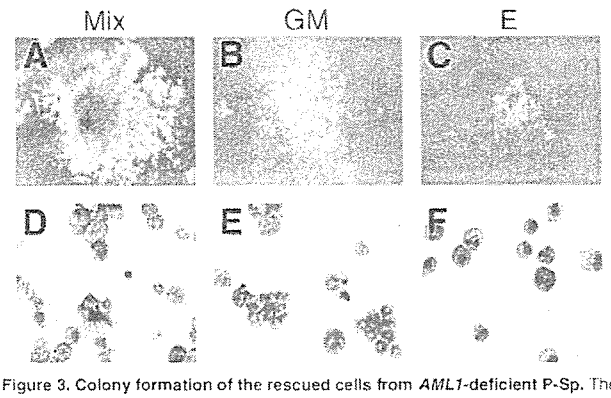

Figure 3. Colony formation of the rescued cells from *AML1*-deficient P-Sp. The hematopoietic defect of *AML1*-deficient P-Sp regions was rescued by retroviral expression of AML1b, and the rescued cells were plated into MethoCult3434 medium. The rescued cells generated various types of hematopoietic colonies including definitive origins. Representative hematopoietic colonies by 7 days of culture are shown. (A-C) Morphology of the colonies. (D-F) Cytospin preparation of corresponding cell populations. Cytospins were stained with Wright-Giemsa. Mix indicates mixed colony; GM, granulocyte/macrophage colony; and E, erythroid colony. Photographs were taken with a Nikon Eclipse TE2000-U (Nikon Sankei) at a magnification of × 100.

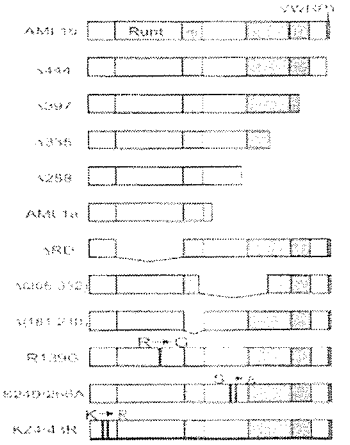

Figure 4. Structures of AML1 and its mutants. The structures of various AML1 mutants are presented schematically. Runt indicates the Runt domain; AD, *trans*-activation domain; ID, inhibitory domain; VWRPY, VWRPY motif; m, a binding region for mSin3A. R→G means a missense mutation at codon 139, which lead to a change of amino acid (R139G, single-letter amino acid code). S→A means a missense mutation at codon 249 and 266, which lead to changes of amino acids (S249A and S266A). K→R means a missense mutation at codon 24 and 43, which lead to changes of amino acid (K24R and K43R).

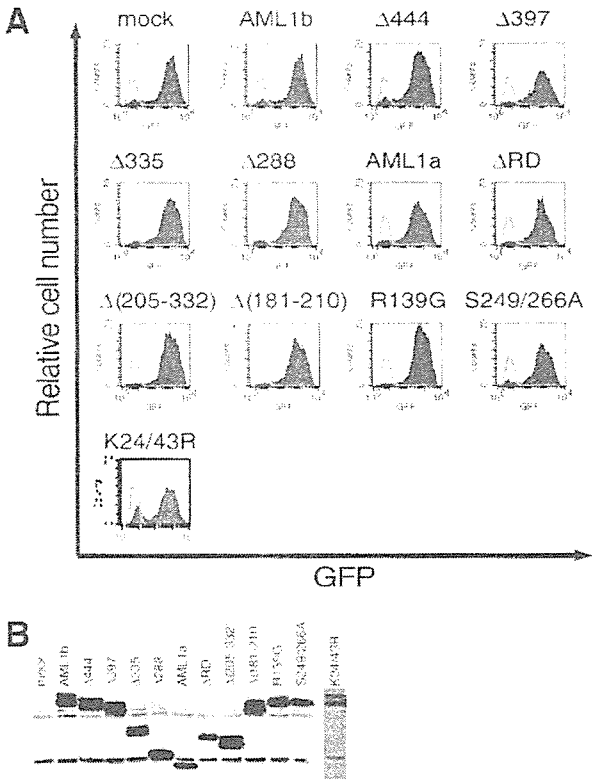

Figure 5. Infection efficiencies of retroviruses expressing AML1 or its mutants. (A) The efficiency of retrovirus-mediated gene transfer of AML1 or its mutants was estimated by infecting NIH3T3 cells. Retrovirus-infected cells were evaluated by the expression of GFP (shaded histograms). Also shown are the noninfected NIH3T3 cells (open histograms). All the retroviruses infected more than 80% of NIH3T3 cells. (B) Expression of AML1 or its mutant proteins in infected NIH3T3 cells. The expression is monitored by immunoblotting of whole-cell lysates with anti-AML1.

enhancement of the transcriptional activity. Finally, AML1b-K24/43R is an acetylation-defective mutant, in which the 2 lysine residues were substituted with arginines. Remarkably, all of these mutants retained the ability to rescue the hematopoietic defect in contrast to the mutants of the Runt domain (Figure 6H,J,K). The cells rescued by these AML1 mutants contained CFCs, expressed hematopoietic cell surface markers, and were morphologically indistinguishable from the rescued cells by wild-type AML1b (data not shown). From these findings, we concluded that the hematopoietic potential of AML1 does not require the interaction with mSin3A, ERK-dependent phosphorylation, or p300-mediated acetylation. Some posttranslational modifications, as well as repressor activities, of AML1 may not necessarily be required for early hematopoietic development. Given that all of these mutants retain a basal activity of gene transcription,[20,42,43] however, these results again argue a close correlation between the transcriptional activity of AML1 and its hematopoietic potential.

Runx2/AML3 and Runx3/AML2 have the capacity to rescue the hematopoietic defect of *AML1*-deficient P-Sp regions

In addition to AML1, there are 2 other known mammalian Runx transcription factors, Runx2/AML3 and Runx3/AML2. To determine whether these Runx proteins have the capacity to substitute for AML1 in hematopoiesis, we infected *AML1*-deficient P-Sp with retroviruses carrying Runx2/AML3 or Runx3/AML2. The infection efficiency and protein expression were assessed by the same method used for AML1 mutants (Figure 7A-B). Interestingly, enforced expression of either Runx2 or Runx3 in *AML1*-deficient P-Sp resulted in the generation of numerous hematopoietic cells (Figure 7C). There is no difference among the rescued hematopoietic cells by all 3 Runx proteins in terms of morphology, expression of surface markers, and CFC activity (data not shown). These results suggest redundant roles among Runx proteins in early hematopoietic development.

Discussion

The striking phenotype of *AML1*-deficient mice has demonstrated an essential role for AML1 in the formation of definitive hematopoiesis during development. However, domain contribution of AML1 in early hematopoietic development has not yet been fully elucidated. Here we described an assay for AML1 function based on the ability to rescue hematopoiesis from the *AML1*-deficient P-Sp regions. Using this system, we found that the hematopoietic potential of AML1 was closely related to its transcriptional activity. Among those mutants used in this study, AML1bΔ444, AML1bΔ397, and AML1bΔ(181-210) are transcriptionally active in a luciferase assay (Kurokawa et al[41]; data not shown). AML1b-S249/266A and AML1b-K24/43R also retain a basal activity of gene transcription. All of these transcriptionally active mutants of AML1 could confer hematopoietic activity on *AML1*-deficient P-Sp regions. On the contrary, other mutants that lose the transcriptional activation ability (Lutterbach et al.[20] Kurokawa et al[41]; data

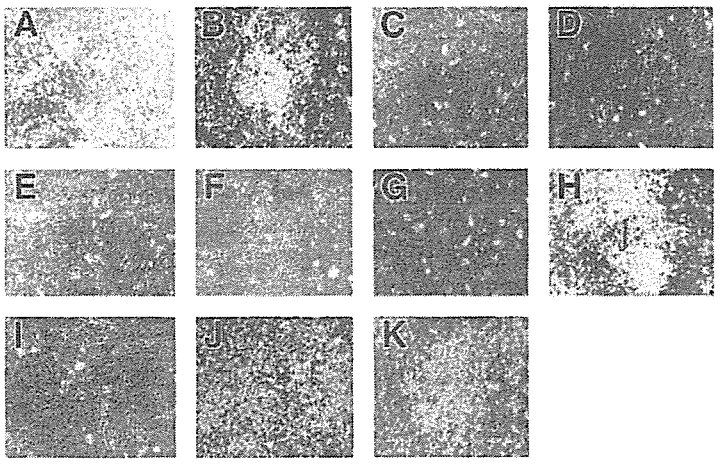

Figure 6. Hematopoietic potential of the AML1 mutants. Cells isolated from *AML1*-deficient P-Sp regions were infected with retrovirus containing the AML1 mutants. Each retrovirus contained (A) AML1bΔ444, (B) AML1bΔ397, (C) AML1bΔ335, (D) AML1bΔ288, (E) AML1a, (F) AML1bΔRD, (G) AML1bΔ(205-332), (H) AML1bΔ(181-210), (I) AML1b-R139G, (J) AML1b-S249/266A, or (K) AML1b-K24/43R. AML1bΔ444 (A), AML1bΔ397 (B), AML1bΔ(181-210) (H), AML1b-S249/266A (J), and AML1b-K24/43R (K) retain the ability to rescue the hematopoietic defect of *AML1*-deficient P-Sp regions, whereas other mutants do not. Shown are phase-contrast microscopic views of these cultures at 14 days. Photographs were taken with a Nikon Eclipse TE2000-U (Nikon Sankei) at a magnification of × 100.

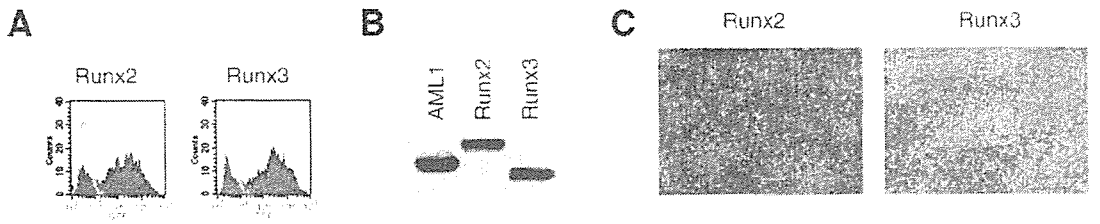

Figure 7. Runx2/AML3 and Runx3/AML2 have the capacity to rescue the hematopoietic defect of *AML1*-deficient P-Sp regions. (A) The efficiency of retrovirus-mediated gene transfer of Runx2/AML3 or Runx3/AML2 was estimated by infecting NIH3T3 cells. Retrovirus-infected cells were evaluated by the expression of GFP (shaded histograms). Also shown are the noninfected NIH3T3 cells (open histograms). (B) Expression of 3 Runx proteins (AML1, Runx2/AML3, and Runx3/AML2) in infected NIH3T3 cells. The expression is monitored by immunoblotting of whole-cell lysates with anti-Flag. (C) Both Runx2/AML3 and Runx3/AML2 have the capacity to rescue the hematopoietic defect of *AML1*-deficient P-Sp regions. Shown are phase-contrast microscopic views of these cultures at 14 days visualized using a Nikon Eclipse TE2000-U (Nikon Sankei) at a magnification of × 100.

not shown) did not rescue the hematopoietic defect. Previously, the C-terminal deletion mutants of AML1b were analyzed with the ES cell culture system. Among them, the mutants containing *trans*-activation subdomains retained the hematopoietic potential.[35] In the present study, we extended these analyses by examining various AML1 mutants and clearly demonstrated that the transcriptional activity of AML1 is essential for in vitro hematopoietic rescue of *AML1*-deficient P-Sp regions.

AML1 can also function as a transcriptional repressor depending on the target gene and the cellular context by recruiting corepressors, such as transduction-like enhancer of split (TLE) and mSin3A. Of these, TLE interacts with AML1 by recognizing its C-terminal VWRPY motif,[21-23] and mSin3A interacts mainly through the region between amino acids 181 and 210.[20] As shown in the current study, the deletion mutants of AML1 that do not interact with these corepressors retained the hematopoietic potential. Therefore, repressor activity of AML1 appears dispensable in early hematopoietic development. Recently, investigations using T-cell–specific *AML1*-deficient mice demonstrated that AML1 has critical functions during thymocyte development.[47] In addition, the *trans*-repression activity of AML1 was suggested to play a role in early thymocyte development.[36] Therefore, the function of AML1 as a transcriptional repressor should be important for appropriate T-cell differentiation. Because the culture system described here lacks the ability to support T-cell development, we are currently establishing another in vitro culture system to investigate the domain contribution of AML1 in T-cell development.

Although a genetic mutation of AML1 has been found in patients with hematologic malignancies,[12-14] the precise mechanisms of leukemogenesis caused by these mutations remain uncertain. Significant in this regard is our observation that AML1b-R139G, the AML1 mutant found in a MDS patient,[13] has lost the hematopoietic potential. This is the first direct evidence that the point mutation in the *AML1* gene, which was found in a patient with hematologic malignancy, leads to loss of its biologic activity in hematopoiesis. Taken together, this experimental system should contribute to further clarification of the molecular basis for leukemogenesis mediated by subtle mutations in the *AML1* gene.

Our study clearly demonstrated that both Runx2/AML3 and Runx3/AML2 have the capacity to rescue the hematopoietic defect of *AML1*-deficient P-Sp regions. Moreover, we also showed that "human" Runx proteins could substitute for the "murine" AML1 in early hematopoietic development because we used human cDNAs in this study. These results are consistent with the fact that the Runt and the *trans*-activation domains, which are essential for hematopoiesis, are highly conserved among members of mammalian Runx family. Thus, Runx-mediated hematopoietic activity depends on the evolutionarily conserved domains in Runx proteins.

In summary, we established an experimental culture system to efficiently examine the hematopoietic potential of Runx transcription factors. By analysis of the mutants, we precisely mapped the region responsible for the hematopoietic potential of AML1 and demonstrated that the transcriptional activity of AML1 is essential for early hematopoietic development. Furthermore, our results suggest a functional redundancy of mammalian Runx proteins in hematopoiesis.

Acknowledgments

We thank M. Ohki for the gift of the human AML1 cDNA, Y. Ito for the human Runx2/AML3 and Runx3/AML2 cDNAs, T. Kitamura for the Plat-E packaging cells and pMY/IRES-EGFP retrovirus vector, T. Nakano for the OP9 stromal cells, and Kirin Brewery Pharmaceutical Research Laboratory for cytokines.

References

1. Kania MA, Bonner AS, Duffy JB, Gergen JP. The Drosophila segmentation gene runt encodes a novel nuclear regulatory protein that is also expressed in the developing nervous system. Genes Dev. 1990;4:1701-1713.
2. Kagoshima H, Shigesada K, Satake M, et al. The Runt domain identifies a new family of heteromeric transcriptional regulators. Trends Genet. 1993;9:338-341.
3. Ogawa E, Maruyama M, Kagoshima H, et al. PEBP2/PEA2 represents a family of transcription factors homologous to the products of the Drosophila runt gene and the human AML1 gene. Proc Natl Acad Sci U S A. 1993;90:6859-6863.
4. Wang S, Wang Q, Crute BE, Melnikova IN, Keller SR, Speck NA. Cloning and characterization of subunits of the T-cell receptor and murine leukemia virus enhancer core-binding factor. Mol Cell Biol. 1993;13:3324-3339.
5. Sasaki K, Yagi H, Bronson RT, et al. Absence of fetal liver hematopoiesis in mice deficient in transcriptional coactivator core binding factor beta. Proc Natl Acad Sci U S A. 1996;93:12359-12363.
6. Wang Q, Stacy T, Miller JD, et al. The CBFbeta subunit is essential for CBFalpha2 (AML1) function in vivo. Cell. 1996;87:697-708.
7. Niki M, Okada H, Takano H, et al. Hematopoiesis in the fetal liver is impaired by targeted mutagenesis of a gene encoding a non-DNA binding subunit of the transcription factor, polyomavirus enhancer binding protein 2/core binding factor. Proc Natl Acad Sci U S A. 1997;94:5697-5702.
8. Miyoshi H, Shimizu K, Kozu T, Maseki N, Kaneko Y, Ohki M. t(8;21) breakpoints on chromosome 21 in acute myeloid leukemia are clustered within a limited region of a single gene, AML1. Proc Natl Acad Sci U S A. 1991;88:10431-10434.
9. Ohki M. Molecular basis of the t(8;21) translocation in acute myeloid leukaemia. Semin Cancer Biol. 1993;4:369-375.
10. Look AT. Oncogenic transcription factors in the human acute leukemias. Science. 1997;278:1059-1064.
11. Kurokawa M, Hirai H. Role of AML1/Runx1 in the pathogenesis of hematological malignancies. Cancer Sci. 2003;94:641-646.
12. Osato M, Yanagida M, Shigesada K, Ito Y. Point mutations of the RUNX1/AML1 gene in sporadic and familial myeloid leukemias. Int J Hematol. 2001;74:245-251.
13. Imai Y, Kurokawa M, Izutsu K, et al. Mutations of

the AML1 gene in myelodysplastic syndrome and their functional implications in leukemogenesis. Blood. 2000;96:3154-3160.

14. Harada H, Harada Y, Niimi H, Kyo T, Kimura A, Inaba T. High incidence of somatic mutations in the AML1/RUNX1 gene in myelodysplastic syndrome and low blast percentage myeloid leukemia with myelodysplasia. Blood. 2004;103:2316-2324.
15. Okuda T, van Deursen J, Hiebert SW, Grosveld G, Downing JR. AML1, the target of multiple chromosomal translocations in human leukemia, is essential for normal fetal liver hematopoiesis. Cell. 1996;84:321-330.
16. Wang Q, Stacy T, Binder M, Marin-Padilla M, Sharpe AH, Speck NA. Disruption of the Cbfa2 gene causes necrosis and hemorrhaging in the central nervous system and blocks definitive hematopoiesis. Proc Natl Acad Sci U S A. 1996;93:3444-3449.
17. Miyoshi H, Ohira M, Shimizu K, et al. Alternative splicing and genomic structure of the AML1 gene involved in acute myeloid leukemia. Nucleic Acids Res. 1995;23:2762-2769.
18. Kanno T, Kanno Y, Chen LF, Ogawa E, Kim WY, Ito Y. Intrinsic transcriptional activation-inhibition domains of the polyomavirus enhancer binding protein 2/core binding factor alpha subunit revealed in the presence of the beta subunit. Mol Cell Biol. 1998;18:2444-2454.
19. Kitabayashi I, Yokoyama A, Shimizu K, Ohki M. Interaction and functional cooperation of the leukemia-associated factors AML1 and p300 in myeloid cell differentiation. EMBO J. 1998;17:2994-3004.
20. Lutterbach B, Westendorf JJ, Linggi B, Isaac S, Seto E, Hiebert SW. A mechanism of repression by acute myeloid leukemia-1, the target of multiple chromosomal translocations in acute leukemia. J Biol Chem. 2000;275:651-656.
21. Aronson BD, Fisher AL, Blechman K, Caudy M, Gergen JP. Groucho-dependent and -independent repression activities of Runt domain proteins. Mol Cell Biol. 1997;17:5581-5587.
22. Imai Y, Kurokawa M, Tanaka K, et al. TLE, the human homolog of groucho, interacts with AML1 and acts as a repressor of AML1-induced transactivation. Biochem Biophys Res Commun. 1998;252:582-589.
23. Levanon D, Goldstein RE, Bernstein Y, et al. Transcriptional repression by AML1 and LEF-1 is mediated by the TLE/Groucho corepressors. Proc Natl Acad Sci U S A. 1998;95:11590-11595.
24. Orkin SH. Development of the hematopoietic system. Curr Opin Genet Dev. 1996;6:597-602.
25. Godin IE, Garcia-Porrero JA, Coutinho A, Dieterlen-Lievre F, Marcos MA. Para-aortic splanchnopleura from early mouse embryos contains B1a cell progenitors. Nature. 1993;364:67-70.
26. Cumano A, Dieterlen-Lievre F, Godin I. Lymphoid potential, probed before circulation in mouse, is restricted to caudal intraembryonic splanchnopleura. Cell. 1996;86:907-916.
27. Muller AM, Medvinsky A, Strouboulis J, Grosveld F, Dzierzak E. Development of hematopoietic stem cell activity in the mouse embryo. Immunity. 1994;1:291-301.
28. Medvinsky A, Dzierzak E. Definitive hematopoiesis is autonomously initiated by the AGM region. Cell. 1996;86:897-906.
29. North T, Gu TL, Stacy T, et al. Cbfa2 is required for the formation of intra-aortic hematopoietic clusters. Development. 1999;126:2563-2575.
30. North TE, de Bruijn MF, Stacy T, et al. Runx1 expression marks long-term repopulating hematopoietic stem cells in the midgestation mouse embryo. Immunity. 2002;16:661-672.
31. de Bruijn MF, Speck NA, Peeters MC, Dzierzak E. Definitive hematopoietic stem cells first develop within the major arterial regions of the mouse embryo. EMBO J. 2000;19:2465-2474.
32. Yokomizo T, Ogawa M, Osato M, et al. Requirement of Runx1/AML1/PEBP2alphaB for the generation of haematopoietic cells from endothelial cells. Genes Cells. 2001;6:13-23.
33. Mukouyama Y, Hara T, Xu M, et al. In vitro expansion of murine multipotential hematopoietic progenitors from the embryonic aorta-gonad-mesonephros region. Immunity. 1998;8:105-114.
34. Takakura N, Watanabe T, Suenobu S, et al. A role for hematopoietic stem cells in promoting angiogenesis. Cell. 2000;102:199-209.
35. Okuda T, Takeda K, Fujita Y, et al. Biological characteristics of the leukemia-associated transcriptional factor AML1 disclosed by hematopoietic rescue of AML1-deficient embryonic stem cells by using a knock-in strategy. Mol Cell Biol. 2000;20:319-328.
36. Nishimura M, Fukushima-Nakase Y, Fujita Y, et al. VWRPY motif-dependent and -independent roles of AML1/Runx1 transcription factor in murine hematopoietic development. Blood. 2004;103:562-570.
37. Nakano T, Kodama H, Honjo T. Generation of lymphohematopoietic cells from embryonic stem cells in culture. Science. 1994;265:1098-1101.
38. Ichikawa M, Asai T, Saito T, et al. AML-1 is required for megakaryocytic maturation and lymphocytic differentiation, but not for maintenance of hematopoietic stem cells in adult hematopoiesis. Nat Med. 2004;10:299-304.
39. Kumano K, Chiba S, Kunisato A, et al. Notch1 but not Notch2 is essential for generating hematopoietic stem cells from endothelial cells. Immunity. 2003;18:699-711.
40. Kitamura T, Koshino Y, Shibata F, et al. Retrovirus-mediated gene transfer and expression cloning: powerful tools in functional genomics. Exp Hematol. 2003;31:1007-1014.
41. Kurokawa M, Tanaka T, Tanaka K, et al. Overexpression of the AML1 proto-oncoprotein in NIH3T3 cells leads to neoplastic transformation depending on the DNA-binding and transactivational potencies. Oncogene. 1996;12:883-892.
42. Tanaka T, Kurokawa M, Ueki K, et al. The extracellular signal-regulated kinase pathway phosphorylates AML1, an acute myeloid leukemia gene product, and potentially regulates its transactivation ability. Mol Cell Biol. 1996;16:3967-3979.
43. Yamaguchi Y, Kurokawa M, Imai Y, et al. AML1 is functionally regulated through p300-mediated acetylation on specific lysine residues. J Biol Chem. 2004;279:15630-15638.
44. Morita S, Kojima T, Kitamura T. Plat-E: an efficient and stable system for transient packaging of retroviruses. Gene Ther. 2000;7:1063-1066.
45. Mukouyama Y, Chiba N, Hara T, et al. The AML1 transcription factor functions to develop and maintain hematogenic precursor cells in the embryonic aorta-gonad-mesonephros region. Dev Biol. 2000;220:27-36.
46. Imai Y, Kurokawa M, Yamaguchi Y, et al. The corepressor mSin3A regulates phosphorylation-induced activation, intranuclear location, and stability of AML1. Mol Cell Biol. 2004;24:1033-1043.
47. Taniuchi I, Osato M, Egawa T, et al. Differential requirements for Runx proteins in CD4 repression and epigenetic silencing during T lymphocyte development. Cell. 2002;111:621-633.

Functional Domains of Runx1 Are Differentially Required for CD4 Repression, TCRβ Expression, and CD4/8 Double-Negative to CD4/8 Double-Positive Transition in Thymocyte Development[1]

Masahito Kawazu,*† Takashi Asai,* Motoshi Ichikawa,* Go Yamamoto,* Toshiki Saito,* Susumu Goyama,* Kinuko Mitani,¶ Kohei Miyazono,† Shigeru Chiba,*‡ Seishi Ogawa,*§ Mineo Kurokawa,[2]* and Hisamaru Hirai*‡

Runx1 (AML1) has multiple functions in thymocyte development, including CD4 repression in immature thymocytes, expression of TCRβ, and efficient β-selection. To determine the functional domains of Runx1 important for thymocyte development, we cultured Runx1-deficient murine fetal liver (FL) cells on OP9-Delta-like 1 murine stromal cells, which express Delta-like 1 and support thymocyte development in vitro, and introduced Runx1 or C-terminal-deletion mutants of Runx1 into the FL cells by retrovirus infection. In this system, Runx1-deficient FL cells failed to follow normal thymocyte development, whereas the introduction of Runx1 into the cells was sufficient to produce thymocyte development that was indistinguishable from that in wild-type FL cells. In contrast, Runx1 mutants that lacked the activation domain necessary for initiating gene transcription did not fully restore thymocyte differentiation, in that it neither repressed CD4 expression nor promoted the CD4/8 double-negative to CD4/8 double-positive transition. Although the C-terminal VWRPY motif-deficient mutant of Runx1, which cannot interact with the transcriptional corepressor Transducin-like enhancer of split (TLE), promoted the double-negative to double-positive transition, it did not efficiently repress CD4 expression. These results suggest that the activation domain is essential for Runx1 to establish thymocyte development and that Runx1 has both TLE-dependent and TLE-independent functions in thymocyte development. *The Journal of Immunology,* **2005, 174: 3526–3533.**

Runx1 (also called *AML1*, *Pebpa2b*, or *Cbfa2*) encodes a member of a family of runt transcription factors that was first identified in humans as a gene that is disrupted in t(8;21) acute myeloid leukemia (1). Homozygous disruption of *Runx1* in mice revealed that Runx1 plays an essential role in definitive hematopoiesis (2, 3). Furthermore, it has been suggested from the very beginning of its cloning that Runx1 also plays roles during thymocyte development (4–6). Runx1, together with other cofactors, binds to the enhancers of *TCR*α (7), β (8), γ (9), and δ (10) and activates transcription of these genes. Runx1 is expressed during thymocyte development as demonstrated by Northern blotting, as well as in situ hybridization of mRNA (11, 12). It is mainly expressed in cortical thymocytes (13), and quantitative real-time PCR of reverse-transcribed RNA revealed that Runx1 mRNA is abundant in CD4/CD8 double-negative (DN)[3] thymocytes (14). When Runx1 was overexpressed in thymocytes using a transgenic system, it was shown to induce CD8 single-positive (SP) thymocyte differentiation (15) and to inhibit the differentiation of Th2 effector T cells (16). Recently, we found that T cell-specific disruption of *Runx1* in mice using the *Cre-loxP* recombinase system results in a profound defect in the DN to CD4/8 double-positive (DP) transition,[4] and others also demonstrated that Runx1 actively represses *CD4* expression in DN thymocytes (14). Together, these findings confirm that Runx1 plays an essential role in early thymocyte development. In view of its functions in T cell development, it is noteworthy that the *Runx1* gene is disrupted in t(4;21)(q28;q22) found in T cell acute lymphoblastic leukemia (17, 18).

Runx1 has several distinct domains of defined biochemical functions. The Runt domain mediates both binding to DNA and dimerization with core-binding factor β subunit (4), whereas the activation domain interacts with transcriptional coactivators to upregulate transcription of the target genes (19, 20). Toward the C terminus of the activation domain lies an inhibitory domain that counteracts the effect of the activation domain (21). Furthermore,

Departments of *Hematology and Oncology, †Molecular Pathology, ‡Cell Therapy and Transplantation Medicine, and §Regeneration Medicine for Hematopoiesis, Graduate School of Medicine, University of Tokyo, Tokyo, Japan; and ¶Department of Hematology, Dokkyo University School of Medicine, Tochigi, Japan

Received for publication September 22, 2004. Accepted for publication January 4, 2005.

The costs of publication of this article were defrayed in part by the payment of page charges. This article must therefore be hereby marked *advertisement* in accordance with 18 U.S.C. Section 1734 solely to indicate this fact.

[1] This work was supported in part by Grants-in-Aid for Scientific Research from KAKENHI (14370300, 13218021, 13557080, and 16·61610), Special Coordination Funds for Promoting Science and Technology from the Ministry of Education, Culture, Sports, Science and Technology, the Japanese Government, and Research on Human Genome and Tissue Engineering, Health and Labor Sciences Research Grants from the Ministry of Health, Labour and Welfare of Japan, H14-GENOME-006.

[2] Address correspondence and reprint requests to Dr. Mineo Kurokawa, Department of Hematology and Oncology, Graduate School of Medicine, University of Tokyo, 7-3-1 Hongo, Bunkyo-Ku, Tokyo 113-8655, Japan. E-mail address: kurokawa-tky@umin.ac.jp

[3] Abbreviations used in this paper: DN, double-negative; SP, single-positive; DP, double-positive; TLE, Transducin-like enhancer of split; FTOC, fetal thymus organ culture; FL, fetal liver; tg, transgenic; rh, recombinant human; cko, conditionally knocked out; ctrl, control.

[4] T. Asai, T. Yamagata, T. Saito, M. Ichikawa, S. Seo, G. Yamamoto, K. Maki, K. Mitani, H. Oda, S. Chiba, et al. Runx1 is required for integrity of the pre-T cell receptor complex and Lck kinase activity in early thymocyte development. *Submitted for publication.*

0022-1767/05/$02.00

the C-terminal VWRPY motif, which mediates the interaction with Transducin-like enhancer of split (TLE), a transcriptional corepressor (22, 23) (see Fig. 3*A*), and a domain which represses *p21* transcription through the interaction with mammalian Sim3 isoform A corepressor (24) (not shown in Fig. 3*A*) are also known. Runx1 activates the transcription of different genes by interacting with different cofactors in various types of cells (25). To elucidate the mechanism by which Runx1 exerts various functions, the contributions of each domain to a particular function of Runx1 have been evaluated. Okuda et al. (26) examined the ability of full-length and mutant *Runx1* genes to rescue the hemopoietic defect in Runx1-deficient embryonic stem cells through a knock-in approach and demonstrated that the activation domain, but not the VWRPY motif, is indispensable for definitive hematopoiesis. No alterations in thymocyte subpopulations were detected in mice in which the VWRPY motif of Runx1 is genetically disrupted, although they have a significantly small thymus (27). In their study, the roles of the activation domain during thymocyte development were not assessed, due to a profound defect in hematopoiesis in the absence of the activation domain of Runx1. Therefore, the roles of functional domains of Runx1 in thymocyte development have not yet been adequately clarified.

Although fetal thymus organ culture (FTOC) has been conventionally used for in vitro studies on thymocyte development (28), it is difficult to achieve high gene-transduction efficiency and to obtain a sufficient number of cells for analyses with FTOC. We used an in vitro culture system in which fetal liver (FL) cells from wild-type mouse embryos follow normal thymocyte development on a layer of OP9-Delta-like 1 (DL1) murine stromal cells expressing a Notch ligand, DL1, on their surface (29, 30). In this system, FL cells from Runx1-deficient embryos exhibited defective thymocyte development, which was successfully restored by the reintroduction of full-length Runx1 by retroviral infection. We also introduced several forms of Runx1 mutants into the Runx1-deficient FL cells and evaluated their ability to restore thymocyte development, which revealed distinct functions of Runx1 domains during thymocyte development.

Materials and Methods

Preparation of cDNAs of Runx1 mutants and gene transduction

cDNAs of C-terminal deletion mutants of Runx1, Δ447, Δ372, Δ320, and Δ291, with a *Not*I site on their 5′ terminus and an *Xho*I site on their 3′ terminus, were PCR amplified from template murine *Runx1* cDNA (a gift from M. Satake, Tohoku University, Sendai, Japan) using *TaKaRa LA taq* (Takara Bio) with the following sets of primers: a sense oligonucleotide for all constructs, 5′-AAAAGCGGCCGCATCGATACCATGCGTATCCCC GT-3′; antisense oligonucleotides: *Δ447*, 5′-TTTTCTCGAGTCAGGC CTCCTCCAGGCGCGCGGG-3′; *Δ372*, 5′-TTTTCTCGAGTCAGCCGG TCTGGAAGGGCCCGGC-3′; *Δ320*, 5′-TTTTCTCGAGTCAGCGCGGG TCGGAGATGGACG-3′; and *Δ291*, 5′-TTTTCTCGAGTCAAAGTT CTGCAGAGAGGCTGG-3′. Each PCR product was digested with *Not*I and *Xho*I and cloned into the *Not*I-*Xho*I site, 5′ upstream of internal ribosomal entry site-*GFP* of the *pGCDNsam* (a gift from H. Nakauchi, Tokyo University, Tokyo, Japan) retrovirus vector (31). Nucleotide sequences of these mutant plasmids were confirmed using the ABI Ready Reaction Dye Terminator Cycle Sequencing kit and ABI3100 semiautomated sequencers (Applied Biosystems). To obtain retrovirus-producing cells, ψMP34 packaging cells (a gift from Wakunaga Pharmaceutical) were transfected with these retrovirus plasmids, followed by single cell sorting for GFP with a FACSVantage (BD Biosciences). To characterize cells transduced with retrovirus plasmids, GFP-positive cells were gated and analyzed.

Cell preparation and genotyping

Embryos at 14.5 days postcoitus (E14.5) were obtained by mating $Runx1^{+/-}$ mice (female) and $Runx1^{floxed/+}$, *Lck-Cre* transgenic (tg)$^+$ mice (male), both of which had been backcrossed for nine generations to C57BL/6. *Lck-Cre* tg mice were kindly provided by J. Takeda (Osaka University, Osaka, Japan) (32). FLs were dissected from the E14.5 embryos and then subjected to single cell suspension by pipetting. An aliquot of the FL cell suspension was subjected to DNA extraction followed by genotyping using PCR with primers *f2* (5′-ACAAAACCTAGGTGTAC CAGGAGAACAAGT-3′), *f120* (5′-CCCTGAAGACAGGAGAAGTTT CCA-3′), and *r1* (5′-GTCTACTCCTTGCCTCAGAAAACAAAAAC-3′), in which floxed and floxed-out (or deleted) alleles were amplified as 280-bp (f120-r1) and 220-bp (f2-r1) PCR fragments, respectively.

Culture of FL cells on OP9-DL1 stromal cells

FL cells were cultured on OP9-DL1 cells (generous gifts from J.C. Zúñiga-Pflücker, University of Toronto, Toronto, Canada) (29) according to the original descriptions with minor modifications. In brief, mononuclear cells were separated from a single cell suspension of E14.5 embryos of C57BL/6 mice by centrifugation on a Ficoll-Hypaque (AXIS-SHIELD; Lymphoprep) gradient. A total of 5×10^4 mononuclear cells, without further purification of hemopoietic progenitor cells, was cultured on confluent OP9-DL1 cells in flat-bottom 24-well culture plates with 500 μl of MEM (Invitrogen Life Technologies) supplemented with 20% FCS, penicillin/streptomycin, and 5 ng/ml recombinant human (rh) IL-7 (R&D Systems). After 5 days of culture, 5×10^4 cells were passed onto newly prepared OP9-DL1 cells in the presence of 5 ng/ml rhIL-7, and retrovirus infection was performed using polybrene (final concentration 8 μg/ml), followed by another 5 days of culture. A total of 1×10^5 cells were again passed onto newly prepared OP9-DL1 cells and cultured for another 5 days, but in rhIL-7-free culture medium.

Flow cytometry

Cells were collected from culture plates, suspended in PBS, and then incubated with mAbs for 30 min on ice. If necessary, this was followed by additional incubation with the secondary reagents for another 30 min on ice. After being washed with PBS, cells were analyzed by flow cytometry using a FACSCalibur (BD Biosciences) equipped with CellQuest software. All mAbs and fluorochromes used in flow cytometry were purchased from BD Pharmingen: FITC, PE, PerCP, PerCP-CY5.5, allophycocyanin, or Biotin-conjugated CD3ε (500A2), CD4 (RM4-5), CD8a (53-6.7), CD24 (M1/69), CD25 (PC61), CD44 (IM7), CD45.2 (104), CD45R/B220 (RA3-6B2), CD90.2 (Thy1.2; 52-2.1), or TCRβ (H57-597). Intracellular anti-TCRβ allophycocyanin staining was performed using a BD Cytofix/Cytoperm kit (BD Pharmingen) in accordance with the manufacturer's instructions.

Results

Normal FL cells can differentiate into DN and DP thymocytes on OP9-DL1 cells

The ontogenic profiles of nonpurified FL cells on OP9-DL1 cells were essentially similar to those of purified FL cells for hemopoietic progenitor cells ($CD24^{low}$, Lin^-, $Sca\text{-}1^{high}$, CD117/c-Kit^+) (29). Most of the FL cells from wild-type C57BL/6 mouse embryos cultured on OP9-DL1 cells expressed Thy1 without the distinct expression of B220, whereas FL cells cultured on parental OP9 cells did not show a high expression level of Thy1 but had apparently committed to B lymphocytes, as manifested by B220 expression (Fig. 1*A*). After 15 days of culture on OP9-DL1 cells, a considerable number of FL-derived cells became $CD4^+CD8^+$ (Fig. 1*B*) and were thought to correspond to CD4/8 DP thymocytes. These $CD4^+CD8^+$ cells also expressed TCRβ at a level comparable with that in DP thymocytes in adult thymus (Fig. 1*C*), indicating that the FL cells cultured on OP9-DL1 cells in vitro can follow the normal development of DP thymocytes in the thymus. A small number of SP (i.e., $CD4^+CD8^-$ or $CD4^-CD8^+$) cells were also observed, but they expressed only intermediate levels of TCRβ on their cell surface (Fig. 1*C*), suggesting that these cells were not as fully mature as the CD4 SP cells or the CD8 SP cells in the thymus. Another prevalent population in the normal FL cell culture on OP9-DL1 cells was $CD4^-CD8^-$ cells, which were considered to be reminiscent of CD4/CD8 DN thymocytes. DN thymocytes differentiate through the maturation sequences DN1 ($CD44^+CD25^-$), DN2 ($CD44^+CD25^+$), DN3 ($CD44^{low}CD25^-$), and DN4 ($CD44^-CD25^-$) (33), and each DN fraction was detected in FL-derived $CD4^-CD8^-$ cells cultured on OP9-DL1 cells

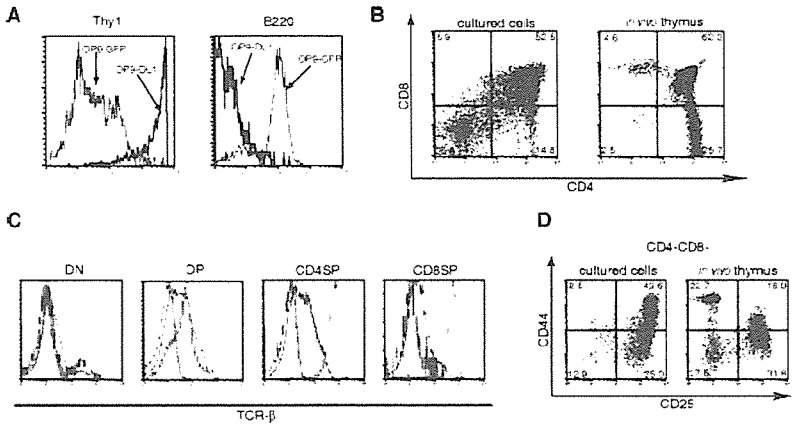

FIGURE 1. FACS analysis of wild-type C57BL/6 FL cells cultured on a stromal layer of OP9 cells that express DL1 (OP9-DL1). *A*, Expression levels of B220 and Thy1 on day 15 in FL cells cultured on an OP9-DL1 layer (thick line) and in FL cells cultured on a control OP9 layer (OP9-GFP; thin line) are shown. Cells were stained with anti-B220 PerCP and anti-Thy1.2 FITC. *B*, CD4/8 expression profile of FL cells cultured on OP9-DL1 for 15 days. The percentage of cells in each quadrant is indicated. *C*, FL cells cultured on OP9-DL1 for 15 days were stained with anti-CD4 PE, anti-CD8 PerCP, and anti-TCRβ allophycocyanin. Expression levels of TCRβ (filled histograms) in each subpopulation, as determined by CD4 and CD8 expression, are shown with the isotype control (blue lines) and expression levels of TCRβ in a corresponding population of adult thymocytes (red lines). *D*, Cells cultured on OP9-DL1 for 15 days were stained with anti-CD4 FITC, anti-CD44 PE, anti-CD8 PerCP, and anti-CD25 allophycocyanin. $CD4^-CD8^-$ cells were gated and their CD25/CD44 expression profile was analyzed. The percentage of cells in each quadrant is indicated.

by staining with CD25 and CD44, although the proportion of cells at the DN2 stage was prominent (Fig. 1*D*).

Phenotypes of Runx1 *conditionally knocked out (cko) FL cells cultured on OP9-DL1 cells*

Using this FL/OP9-DL1 coculture system, FL cells from *Runx1*-targeted (cko: $Runx1^{floxed/-}$, *Lck-Cre* tg) mice were tested for their capacity to differentiate into DP thymocytes. Whereas 10 days of culture of the control (ctrl; $Runx1^{+/+}$, *Lck-Cre* tg) FL cells on OP9-DL1 cells exclusively produced $CD4^-CD8^-$ cells, a similar culture of cko FL cells generated a population that showed an intermediate expression level of CD4 without CD8 ($CD4^{int}CD8^-$) in addition to $CD4^-CD8^-$ cells (Fig. 2*A*). The $CD4^{int}CD8^-$ subset in the cko FL cell culture is thought to be as immature as the $CD4^-CD8^-$ subset because it is quite unlikely that so many cko cells can differentiate beyond DP stage, due to that fact that only a small proportion of ctrl cells progressed to the $CD4^+CD8^+$ cells after 10 days of culture (Fig. 2*A*). Indeed, TCRβ and CD5, whose expression levels rise as thymocytes maturate, were up-regulated in $CD4^+CD8^+$ ctrl cells, but not in $CD4^+CD8^-$ cko cells (Fig. 2*B*). In addition, CD24, whose expression level diminishes as thymocytes maturate, is down-regulated in $CD4^+CD8^+$ ctrl cells, but not in $CD4^+CD8^-$ cko cells (Fig. 2*B*). Furthermore, the expression profile of CD44 and CD25 was comparable with that of $CD4^-CD8^-$ cells (Fig. 2*C*). The extent of Cre-mediated depletion of the floxed *Runx1* allele was greater in $CD4^{int}CD8^-$ cells than in the $CD4^-CD8^-$ cells (Fig. 2*D*), which is consistent with the fact that Runx1 actively represses *CD4* expression in DN thymocytes (14). After 15 days of culture, the ctrl FL cells cultured on OP9-DL1 cells consisted mainly of $CD4^+CD8^+$ and $CD4^-CD8^-$ cells, corresponding to DP and DN thymocytes in the thymus, respectively (Fig. 2*A*). In contrast, cko FL cells cultured for 15 days contained mainly $CD4^-CD8^-$ cells, and only a small fraction were $CD4^+CD8^+$ cells. The $CD4^+CD8^+$ cells from the ctrl FL cell culture showed higher expression levels of TCRβ than did $CD4^-CD8^-$ cells, whereas expression of TCRβ on $CD4^+CD8^+$ cells derived from cko FL cells was as low as that on $CD4^-CD8^-$ cells (data not shown), indicating the impaired maturation of $CD4^+CD8^+$ cells derived from cko FL cells on day 15. These observations are consistent with our unpublished finding in *Runx1* cko mouse, in which TCRβ expression on DP and CD4 SP thymocytes was significantly reduced.[4]

The DN ($CD4^-CD8^-$) population in the ctrl FL-derived cells appeared to contain four subsets of DN1 to DN4 on day 15 of culture (Fig. 2*E*). In contrast, the $CD4^-CD8^-$ population observed in the cko FL cell culture mainly consisted of DN1 and DN2 cells, indicating differentiation arrested at the DN2–3 transition. Thus, on OP9-DL1 cells, ctrl FL cells produced both DN and DP cells in almost the same manner as FL cells from wild-type C57BL/6 mice, whereas thymocyte development from cko FL cells was significantly impaired at the DN2–3 transition and showed the premature expression of CD4.

Runx1 gene transduction can restore the impaired differentiation of Runx1-deficient FL cells

To confirm that the impaired maturation of cko FL-derived cells was caused by a lack of Runx1, we examined whether the reintroduction of Runx1 could rescue the block in the DN2–3 transition found in cko FL-derived cells. The cko FL-derived cells transduced with *Runx1* by retrovirus infection showed a significant increase in DN3 cells accompanied by the appearance of DN4 cells, which was not seen in mock-infected cells (Fig. 3*B*, *top panel*). These results demonstrated that Runx1 is essential for the DN2–3 transition during thymocyte development. Remarkably, when Runx1 was introduced, the control FL cells generated more DN3 and DN4 cells than did mock-infected ctrl FL cells (Fig. 3*B*, *bottom panel*), suggesting that an increased dosage of Runx1 may also affect thymocyte development.

We next sought to determine the functional domains of Runx1 that are involved in thymocyte development. For this purpose, we generated a series of C-terminal deletion mutants of Runx1 (Fig. 3*A*) and transduced them into cko FL cells by retrovirus infection. Infection efficiencies were ~80% as assessed by GFP positivity and were almost constant for all of the constructs (data not shown). Δ447 lacks the C-terminal VWRPY motif, which is required for interaction with TLE (22, 23), whereas Δ372 lacks the inhibitory domain that impedes transcriptional activity mediated by the activation domain of Runx1 (21). The Δ320 mutant lacks a part of the

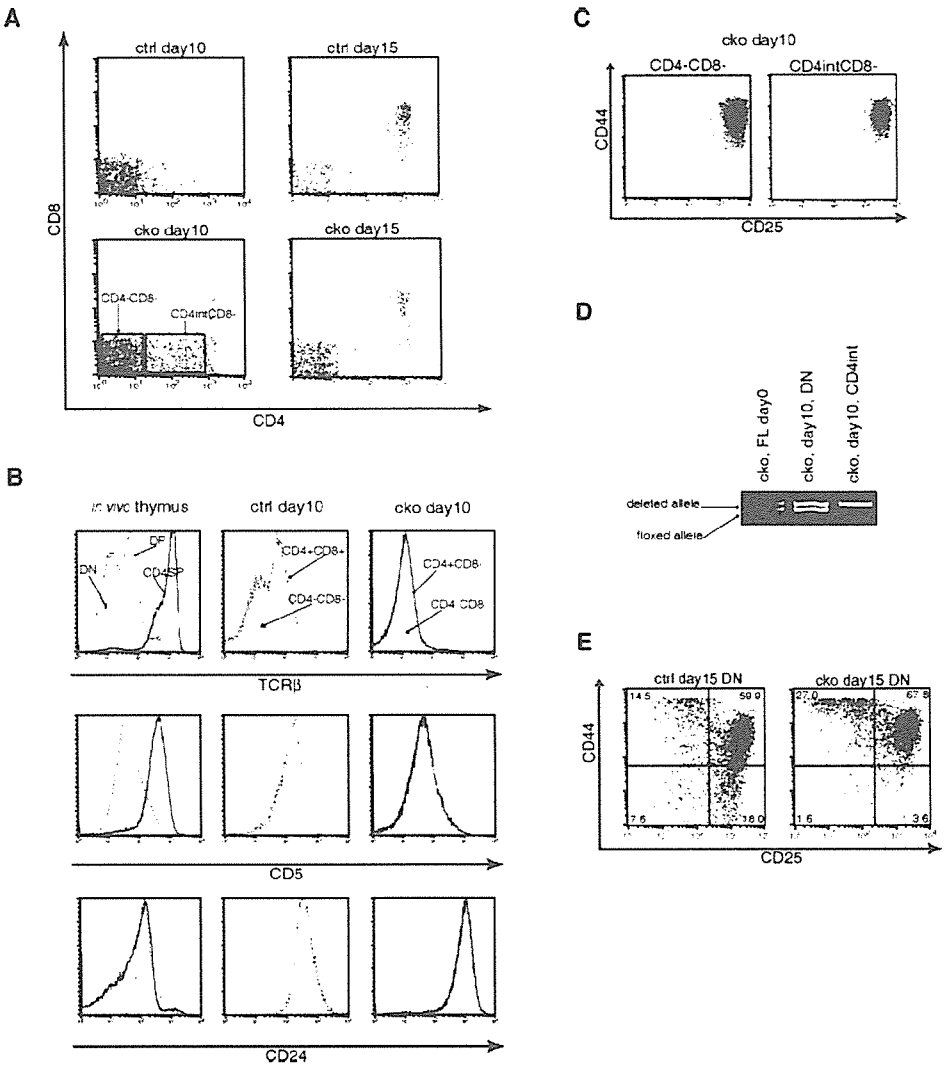

FIGURE 2. FACS analysis of cko FL cells and ctrl FL cells cultured on OP9-DL1. *A*, CD4/CD8 expression profiles of each type of FL-derived cell on days 10 and 15. *B*, Expression levels of TCRβ, CD5, and CD24 in $CD4^+CD8^-$ cko cells (solid lines) and $CD4^+CD8^+$ ctrl cells (dotted lines) cultured for 10 days were compared with those of $CD4^-CD8^-$ cells (gray shades without contour). Those for the indicated subsets of ctrl cells cultured for 10 days and thymocytes derived from adult thymus were also presented. *C*, CD25/CD44 expression profiles of $CD4^-CD8^-$ cells and $CD4^{int}CD8^-$ cells among cko FL cells cultured for 10 days. *D*, Genotype of each subpopulation of cko FL-derived cells, which were sorted with a FACSVantage SE cell sorter (BD Biosciences) after being stained with anti-CD4 PE and anti-CD8 PerCP-CY5.5. Genomic DNA was extracted from sorted cells and electrophoresed after amplification by PCR. *E*, CD25/CD44 expression profiles of $CD4^-CD8^-$ cells on day 15.

activation domain, and Δ291, which completely lacks the activation domain, shows less potent transcriptional activity than does Δ320 (21). The proportions of DN3 and DN4 cells on day 15 of culture were calculated for cko FL-derived cells infected with each mutant (Fig. 3*C*).

Δ*447*-transduced cko FL cells produced DN3 and DN4 cells in numbers comparable with full-length *Runx1*-transduced cko FL cells. Therefore, the VWRPY motif is not necessary for the function of Runx1 in the DN2–3 transition. Although Δ372, which lacks the inhibitory domain, can rescue the DN2–3 transition as efficiently as full-length Runx1, rescue of the DN3–4 transition was still marginally impaired. Despite the fact that the transcriptional activity of Runx1 is derepressed in the absence of the inhibitory domain (21), the differentiation of Δ*372*-transduced cko FL cells is not promoted compared with that of *Runx1*-transduced cko FL cells in this culture system, suggesting that the elevated transcriptional activity does not affect Runx1-dependent thymocyte development.

In contrast, both Δ320 and Δ291, which lack part of and the entire activation domain, respectively, failed to restore either the DN2–3 or DN3–4 transition. Thus, the activation domain is required for the function of Runx1 in the DN2–3 and DN3–4 transitions. Interestingly, the DN3 and DN4 subsets of Δ*320*- or Δ*291*-transduced control FL cells were diminished compared with mock-infected ctrl FL cells (Fig. 3*B*, *bottom panels*), which raises the possibility that both Δ320 and Δ291 suppress the function of endogenous Runx1 in the DN2–3 and DN3–4 transitions in a dominant-negative manner. The suppressive effects of Δ320 and Δ291 were confirmed in three independent experiments (proportions of DN3 cells, $p = 0.031$ for mock vs Δ320 and $p = 0.016$ for mock vs Δ291; proportions of DN4 cells, $p = 0.028$ for mock vs Δ320 and $p = 0.029$ for mock vs Δ291).

To determine the efficiency of Cre-mediated gene deletion in this culture system, genotyping of the *Runx1* alleles was performed for each stage of DN cells. DN3 and DN4 cells were obtained from day 10 culture of *Runx1*-transduced $Runx1^{floxed/floxed}$, *Lck-Cre* tg FL cells. The whole culture on day 5 was used to genotype DN2 cells, because almost all of the cells were at the DN2 stage on day 5. Genomic DNA was extracted from each DN subpopulation and used as a template for genotyping. Only the floxed allele was detected in the FL cells on day 0, whereas both the floxed and deleted alleles were detected in day 5 DN2 cells. In contrast, only the deleted allele was detected from the DN3 and DN4 subsets derived from *Runx1*-transduced FL cells (Fig. 3*D*). These results indicated that Cre-mediated gene deletion was only partially achieved in the DN2 cells, but was complete at the DN3 stage in this culture system.

Because our unpublished observation using *Runx1* cko mice revealed decreased TCRβ expression in Runx1-deficient DN3 thymocytes,[4] we examined expression of intracellular TCRβ in DN

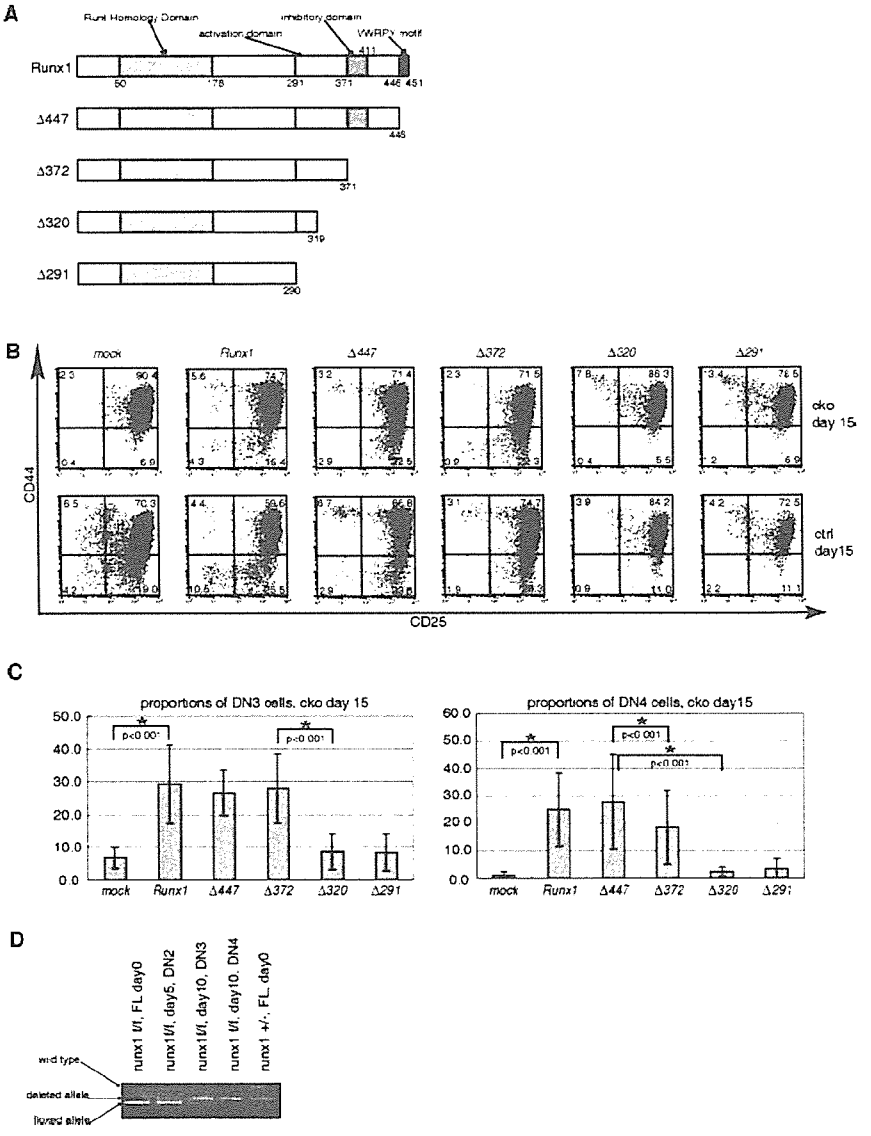

FIGURE 3. Development of DN3 and DN4 cells in FL-derived cells, which were transduced with the genes for Runx1 or its C-terminal deletion mutants. *A*, Construction of Runx1 and C-terminal deletion mutants. Numbers indicate the positions of amino acid residues from the N terminus. *B*, CD25/CD44 expression profile of CD4/CD8 DN cells on day 15 are shown for cko FL-derived cells (*top panels*) and ctrl FL-derived cells (*bottom panels*) with transduced Runx1 mutants. Cells were stained with anti-CD44 PE, anti-CD3 PerCP, anti-CD4 PerCP, anti-CD8 PerCP, and anti-CD25 allophycocyanin. GFP-positive and PerCP-negative cells were gated and analyzed for the CD25/CD44 expression profile. The percentage of cells in each quadrant is indicated. *C*, Proportions (%) of DN3 ($CD44^{low}CD25^{+}$) and DN4 ($CD44^{-}CD25^{-}$) cells on day 15 in nine independent experiments were averaged and are shown with ±1× SE. Asterisks indicate statistically significant differences, and *p* values were indicated. ANOVA and post hoc comparison (Fisher test) were performed using StatView software (SAS Institute). *D*, DN3 and DN4 thymocytes were sorted by a FACSVantage SE cell sorter (BD Biosciences) after being stained by anti-CD3ε PE, anti-CD4 PE, anti-CD8 PE, anti-CD25 PerCP-CY5.5, and anti-CD44 allophycocyanin. Genomic DNA was extracted from the sorted cells and electrophoresed after PCR amplification.

cells in day 15 culture of FL cells. A significant proportion of *Runx1*-transduced cko DN cells expressed intracellular TCRβ, whereas TCRβ was barely detected in mock-infected cko DN cells (Fig. 4). Transduction of *Δ447* or *Δ372* restored intracellular TCRβ expression to a level comparable with that of full-length *Runx1*, whereas cko DN cells transduced with *Δ320* or *Δ291* did not express intracellular TCRβ. In accordance with the increase in the proportions of DN3 and DN4 cells among *Runx1*-transduced ctrl cells (Fig. 3*B*, *bottom*), the percentage of *Runx1*-transduced ctrl DN cells expressing intracellular TCRβ was increased compared with the

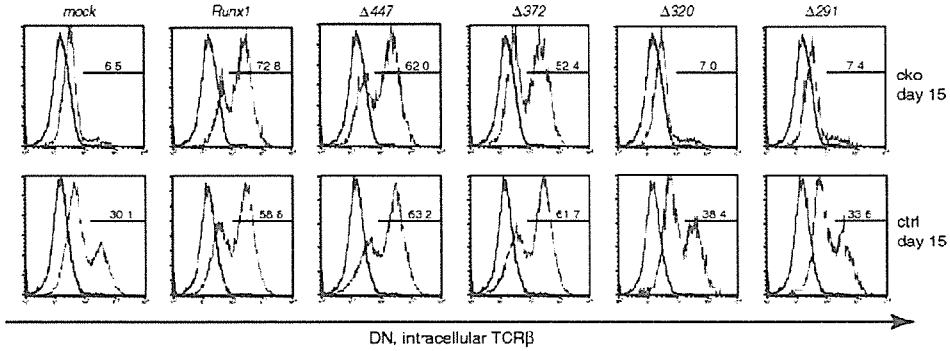

FIGURE 4. Expression levels of intracellular TCRβ in the $CD4^{-}CD8^{-}$ subset among cko (*top panels*) and ctrl (*bottom panels*) FL-derived cells on day 15. Transduced Runx1 mutants are shown above. Cells were stained with anti-CD4 PE, anti-CD8 PerCP, and anti-TCRβ allophycocyanin. GFP-positive, PE-negative, and PerCP-negative cells were analyzed for TCRβ expression (filled histograms). Expression levels of intracellular TCRβ in splenic B cells are overlaid as negative controls (thick lines). The percentages of positive cells are indicated in each histogram.